

Breaking of clustering and macroscopic coherence under the lens of asymmetry measures

Florent Ferro

Université Paris-Saclay, CNRS, LPTMS, 91405, Orsay, France

In one-dimensional systems, spontaneous symmetry breaking (SSB) states are fragile by nature, as the injection of a non-zero energy density above the ground state is expected to restore the symmetry. This instability implies that local perturbations can lead to macroscopic correlation profiles, a breaking of clustering properties and even macroscopic quantum superpositions. In this work, we investigate the effect of interaction on this phenomenology by considering an interacting model with conserved domain wall number, that possesses a ferromagnetic ground state breaking the \mathbb{Z}_2 symmetry of the Hamiltonian. We first show that a local quench in this system amplifies quantum interferences, producing a macroscopic magnetisation profile that directly reflects the scattering phase of the model. Then, we use two asymmetry measures, namely the Entanglement Asymmetry (EA) and Quantum Fisher Information (QFI), to characterise the quantum coherence associated with the fluctuations of the magnetisation. By focusing on subsystems comparable in size to the light-cone of the perturbation, we confirm the emergence of macroscopic quantum coherence throughout the whole perturbed region. Finally, we discuss the link between EA and QFI and show that the variance/EA inequality for pure state can be generalised to a QFI/EA inequality for mixed states.

I. INTRODUCTION

While quantum physics is very efficient to describe the smallest scales of matter, it is still unclear whether genuine quantum phenomena can survive at macroscopic scales. For equilibrium states of systems described by local Hamiltonians, clustering properties ensure that at large distances, different subsystems act independently, leaving no ground for macroscopic quantum superpositions such as the famous "cat states" -or GHZ states [1] - imagined by Schrödinger [2, 3]. The interest in macroscopic quantum effects however came back with the recent breakthroughs in quantum simulators and quantum circuits, in which it is now possible to engineer such superpositions of up to ~ 20 qubits [4–6]. However, the protocols to create such states are fine tuned, and by nature cat states are fragile and unstable: the loss of a single qubit destroys the superposition. Therefore, two questions arise: can macroscopic quantum superpositions emerge from more "natural" scenarios, and if so, can they be more robust than cat states ?

In equilibrium, critical ground states are natural candidates since they possess algebraically decaying correlations, allowing for "enhanced" quantum coherence [7–9]. Out-of-equilibrium, it is natural to directly look for scenarios in which correlations are non-decaying altogether in a given region. This breaking of clustering is typically signalled by magnetization profiles becoming self-similar at different times through a rescaling (ballistic, diffusive...). Such scaling dynamics occur in various settings: local quenches on ferromagnetic ground states [10–12] or quantum scars [13], domain wall melting [14–16], systems with jamming [17, 18], interface physics [19–23]... In particular, in Ref [24] we showed that "robust" macroscopic quantum superpositions can appear after a local quench on the spontaneously symmetry broken (SSB) ground state of the Ising model in the ordered phase. This effect has a very simple interpretation: excitations in the symmetry-broken phase are not local but semi-local, which essentially means that they are semi-classically described by domain walls [25, 26]. The ballistic spreading of the domain wall wavefunctions results in quantum superposition of states with macroscopically different (diverging linearly in time) magnetisations.

These superpositions are robust in the sense that they survive the loss of a part of the system (i.e. considering subsystems), but it is not obvious whether they can survive in presence of interactions, which

induces non-trivial scattering and the formation of bound states. In this paper, we fill this gap and generalise the results of [24] on local quenches to the interacting case. We study quantum fluctuations by explicitly computing two quantities from the resource theory of asymmetry [27], having in mind that an asymmetry with respect to the symmetry group generated by a charge Q essentially quantifies coherence between the charge sectors of Q [28–31].

The first of these tools is the Entanglement asymmetry (EA), also known as G asymmetry [32] or relative entropy of superposition [33] in the field of quantum information. Since its original introduction for the study of the quantum Mpemba effect [34, 35], EA has recently gained a lot of attention in the many-body and high-energy communities [36–58], and has even been measured experimentally [59, 60]. It is now recognised as a standard tool to quantify how much a quantum state breaks a symmetry. By bounding the asymmetry of subsystems of size comparable to the light-cone, we will extract its leading behaviour and show that subsystems fall in quantum superposition of a number of magnetisation sectors that diverges in time.

To complete this analysis, we also compute the Quantum Fisher Information (QFI), and explicitly work out a relation between them through a new bound based on the one between entropy and variance. While the QFI can be used to quantify asymmetry [32, 61–63], it was originally introduced in the context of quantum metrology via the Cramer Rao bound: the QFI determines the maximal precision one can achieve in parameter estimation. Actually, Ref [64] showed that QFI is a probe for resourceful quantum states in a large number of resource theories. One of its main interests relies in the fact that it gives a lower bound to the entanglement depth (the minimum number of multipartite entangled parts of a given state), making it a witness of multipartite entanglement [65–68]. Furthermore, contrary to the latter, QFI is not sensible to infinitesimally small correlations between different parts of the system. For these reasons, it is a sensible probe of multipartite entanglement in many-body physics, and has been used to characterise it both in [9, 69, 70] and out of equilibrium [24, 71]. While the QFI is generally a very complex quantity to evaluate, a lot of techniques have been developed to access it, notably in free-fermionic systems [72–74], and through simpler related quantities such as the Wigner-Yanese-Dyson Skew Information [75], see ref [24]. Furthermore, it can be expressed as a series of experimentally accessible quantities [76], and in thermal states its connection to the susceptibility [69] makes it directly measurable [77].

We use the dual XXZ spin chain [78] - obtained from the XXZ chain via a Kramers-Wanier transformation - as an interacting toy model to study the effect of a local perturbation on an SSB ground state that spontaneously breaks the \mathbb{Z}_2 symmetry of the Hamiltonian. We take advantage of its Coordinate Bethe Ansatz description to solve the dynamics after the quench, and show that, as expected, it breaks the clustering properties on ballistic scales through its transverse magnetisation profile. By "diagonalising" the scattering phase of the model, we make analytical predictions for the scaling limit of the EA and QFI that we compare with exact numerical data, obtained using the low-dimensionality of the accessible Hilbert space after the local quench. We show that interaction does not spoil the phenomenology occurring in free models, and that any subsystem close to the perturbation, with a size scaling with that of the light-cone, falls into robust macroscopic quantum superpositions.

II. SETUP

In this paper, we consider the dual XXZ Hamiltonian [78]:

$$H = \frac{1}{4} \sum_{j=1}^N (\sigma_j^x - \Delta)(1 - \sigma_{j-1}^z \sigma_{j+1}^z) - h \sum_{j=1}^N \sigma_j^z \sigma_{j+1}^z, \quad (1)$$

where we choose to impose periodic boundary conditions (PBC) $\sigma_{N+1}^\alpha = \sigma_1^\alpha$ and we restrict ourselves to $\Delta \geq 0$. By duality with the XXZ model, this Hamiltonian is exactly solvable by Coordinate Bethe Ansatz

[79]. It presents a $U(1)$ symmetry generated by the charge $Q = \frac{1}{2} \sum_{j=1}^N (1 - \sigma_j^z \sigma_{j+1}^z)$, which counts the number of domain walls between ferromagnetic regions of opposite transverse magnetisations. Additionally, the system exhibits a \mathbb{Z}_2 symmetry represented by the spin flip operator $P = \prod_{j=1}^N \sigma_j^x$. In the zero particle sector ($Q = 0$), there are two eigenstates of H corresponding to each eigenvalue of P :

$$|\pm\rangle = \frac{1}{\sqrt{2}} (|\uparrow\rangle^{\otimes N} \pm |\downarrow\rangle^{\otimes N}), \quad (2)$$

such that $P |\pm\rangle = \pm |\pm\rangle$. We can anticipate that for sufficiently high values of h , ferromagnetic interactions dominate and the ground state of H lies in the $Q = 0$ sector. It is easy to see that $|\rangle$ and $|\langle\rangle$ are degenerate, $H |\pm\rangle = 0$, therefore the trivial product states with maximal and minimal transverse magnetisation, $|\uparrow\rangle = |\uparrow\rangle^{\otimes N}$ and $|\downarrow\rangle = |\downarrow\rangle^{\otimes N}$, are also eigenstates of H . These states explicitly break the \mathbb{Z}_2 symmetry of the system.

We are interested in the effect of a local perturbation on the symmetry-broken ground state, $|\uparrow\rangle$. The simplest such perturbation is the creation of a small ferromagnetic domain of neighbouring sites $\llbracket j_1, j_2 \rrbracket = \{j_1, j_1 + 1, \dots, j_2\}$, of size $d_0 = j_2 - j_1 + 1$. Without loss of generality (H is translationally invariant) and assuming d_0 is odd for simplicity, we center this domain around site 0 ($\equiv N$ by PBC). We can thus write the state after the local perturbation as:

$$|\Psi_{d_0}(t)\rangle = e^{-iHt} \prod_{j=-(d_0-1)/2}^{(d_0-1)/2} \sigma_l^x |\uparrow\rangle. \quad (3)$$

Since $[H, Q] = 0$ the state remains in the $Q = 2$ sector at all times. This means that the two domain walls can move and the distance between them can fluctuate, but they cannot be created or annihilated. The physical situation corresponding to this local quench is therefore similar to the one studied in Refs [11, 24], except that the domain walls are not freely propagating but can instead scatter or form bound states.

III. CBA DESCRIPTION

We can explicitly work out the time evolution of the state given by Eq. (3) using coordinate Bethe Ansatz. Let us index the domain wall positions with half integers $l_1, l_2 \in \llbracket \frac{1}{2}, N - \frac{1}{2} \rrbracket$. For $l_1 < l_2$ we define the basis states of the $Q = 2$ sector as:

$$|l_1 l_2\rangle_{\pm} = \frac{1}{\sqrt{2}} (|\cdots \uparrow \uparrow \downarrow_{l_1+1/2} \cdots \downarrow_{l_2-1/2} \uparrow \uparrow \cdots \rangle \pm |\cdots \downarrow \downarrow \uparrow_{l_1+1/2} \cdots \uparrow_{l_2-1/2} \downarrow \downarrow \cdots \rangle), \quad (4)$$

where $P |l_1 l_2\rangle_{\pm} = \pm |l_1 l_2\rangle_{\pm}$. The boundary conditions depend on the parity sector, $|l_1 N + \frac{1}{2}\rangle_{\pm} = \pm |\frac{1}{2} l_1\rangle$, and also allow us to write negative domain wall positions. In this basis the state $|\Psi_{d_0}(t)\rangle$ is expressed as a superposition of states in different parity sectors:

$$|\Psi_{d_0}(t)\rangle = \frac{1}{\sqrt{2}} e^{-iHt} \left(\left| -\frac{d_0}{2}, \frac{d_0}{2} \right\rangle_{+} + \left| -\frac{d_0}{2}, \frac{d_0}{2} \right\rangle_{-} \right). \quad (5)$$

We show in Appendix A that in the thermodynamic limit $N \rightarrow \infty$, for fixed time t and distances between the position of the domain walls, the transition amplitude ${}_s \langle f_1 f_2 | e^{-iHt} | i_1 i_2 \rangle_s$ becomes independant of s and N . The periodic chain is effectively "unwrapped" into an infinite line of origin 0. The indices i_1, i_2, f_1, f_2

remain at a finite distance from the origin, and the paths with non-zero winding number around the chain are suppressed by Lieb-Robinson bounds [80]. Consequently, it makes sense to introduce the states $|l_1 l_2\rangle = \frac{1}{\sqrt{2}}(|l_1 l_2\rangle_+ + |l_1 l_2\rangle_-)$ that, after taking the thermodynamic limit, satisfy

$$\sigma_j^z |l_1 l_2\rangle = \text{sgn}(l_1 - j) \text{sgn}(l_2 - j) |l_1 l_2\rangle. \quad (6)$$

This allows us to write the state at time t as

$$|\Psi_{d_0}(t)\rangle = \sum_{f_1 < f_2 \in \mathbb{Z}} \Psi_{f_1, f_2}^{d_0}(t) |f_1 f_2\rangle. \quad (7)$$

The dynamics of the amplitude $\Psi_{f_1, f_2}^{d_0}(t)$ is governed by two types of excitations: scattering states and bound states. We decompose the total wavefunction as a sum of these two contributions: $\Psi_{f_1, f_2}^{d_0}(t) = \psi_{f_1, f_2}^{d_0}(t) + \nu_{f_1, f_2}^{d_0}(t)$.

a. The first contribution $\psi_{f_1, f_2}^{d_0}(t)$ corresponds pairs of particles with real momenta $k_1, k_2 \in \mathbb{R}$:

$$\psi_{f_1, f_2}^{d_0}(t) = \frac{1}{4\pi^2} \int_{-\pi}^{\pi} dk_1 dk_2 \tilde{\psi}_{d_0}(k_1, k_2) e^{i[k_1(f_1 - d_0/2) + k_2(f_2 + d_0/2)]} e^{-i(\epsilon_{k_1} + \epsilon_{k_2})t}, \quad (8)$$

where $\epsilon_k = h - \cos k$ is the single-particle bare energy, $\tilde{\psi}_{d_0}(k_1, k_2) = e^{id_0(k_1 - k_2)} + S(k_1, k_2)$ and

$$S(k_1, k_2) = -\frac{1 + e^{i(k_1 + k_2)} - 2\Delta e^{ik_1}}{1 + e^{i(k_1 + k_2)} - 2\Delta e^{ik_2}} \quad (9)$$

is the scattering phase of the model. These excitations represent scattering states (analogous to magnons in the XXZ model). Its amplitude is $\mathcal{O}(t^{-1})$ for $|f_1|, |f_2| \leq t$, thus it describes two ferromagnetic domains spreading on a region of size $2t$.

Note that for $\Delta < 1$, this integral expression is ill-defined, but it still makes sense by representing the scattering phase in Fourier space, $S(k_1, k_2) = \sum_{n_1 n_2} S_{nm} e^{i(k_1 n_1 + k_2 n_2)}$, see Appendix D. Under this representation, we can write $\psi_{f_1, f_2}^{d_0}(t)$ as a sum over Bessel functions $J_n(t)$ as

$$\psi_{f_1, f_2}^{d_0}(t) = i^{f_1 + f_2 - l_1 - l_2} J_{f_1 - l_1}(t) J_{f_2 - l_2}(t) + \sum_{mn} i^{m+n} S_{m-f_1+l_2, n-f_2+l_1} J_m(t) J_n(t). \quad (10)$$

This sum can then be cut to discard the contribution coming from the Bessel functions in their exponential decaying region.

b. The other contribution $\nu_{f_1, f_2}^{d_0}(t)$ represents bound states. They correspond to pairs of complex-conjugated momenta $\{K/2 - i\eta(K), K/2 + i\eta(K)\}$ with total momentum K , where $e^{-\eta(K)} = \Delta^{-1} \cos(K/2)$ is the solution of $S(K/2 + i\eta(K), K/2 - i\eta(K)) = 0$. Their contribution to the amplitude reads:

$$\nu_{f_1, f_2}^{d_0}(t) = \frac{1}{2\pi} \int_{-\pi}^{\pi} dK \tilde{\nu}_{f_2 - f_1}^{d_0}(K) e^{iK \frac{f_1 + f_2}{2}} e^{-iE_K t}, \quad (11)$$

where

$$\tilde{\nu}_{d_f}^{d_0}(K) = (e^{-\eta(K)(d_0 + d_f - 2)} - e^{-\eta(K)(d_0 + d_f)}) \theta(\eta(K)), \quad (12)$$

$E_K = \epsilon_{K/2 - i\eta(K)} + \epsilon_{K/2 + i\eta(K)} = 2h - \Delta - \Delta^{-1} \cos^2(K/2)$ and where the Heaviside step function $\theta(\eta(K))$ restricts the integration to states satisfying $|\cos K/2| \leq \Delta$. This condition ensures that the bound-states

wavefunctions are normalisable and that their group velocity, given by $E'_K = \frac{1}{2\Delta} \sin(K)$, does not exceed that of the scattering states (i.e. 1). $\nu_{f_1, f_2}^{d_0}(t)$ is $\mathcal{O}(t^{-1/2})$ and is exponentially decaying in $f_2 - f_1$, therefore it describes a localised ferromagnetic domain of $\mathcal{O}(1)$ size moving through the chain in the light-cone $(-v_B^{\max}t, v_B^{\max}t)$, where the maximal bound state velocity is given by $v_B^{\max} = \max(1, 1/(2\Delta))$.

Using the wavefunctions (8) and (11), we introduce the (unnormalised) states $|\psi_{d_0}(t)\rangle = \sum_{f_1 < f_2 \in \mathbb{Z}} \psi_{f_1 f_2}^{d_0}(t) |f_1 f_2\rangle$ and $|\nu_{d_0}(t)\rangle = \sum_{f_1 < f_2 \in \mathbb{Z}} \nu_{f_1 f_2}^{d_0}(t) |f_1 f_2\rangle$. These states correspond to the projection of $|\Psi_{d_0}(t)\rangle$ onto the sectors associated with pairs of real and complex momenta respectively. H is block diagonal between these two sectors, therefore the norm of these states are constant in time. They are given by

$$p_{d_0}^S = \langle \psi_{d_0}(t) | \psi_{d_0}(t) \rangle = \frac{1}{8\pi^2} \int_{-\pi}^{\pi} dk_1 dk_2 |\tilde{\psi}_{d_0}(k_1, k_2)|^2, \quad (13)$$

and $p_{d_0}^B = 1 - p_{d_0}^S$.

IV. SCALING LIMIT OF THE TRANSVERSE MAGNETISATION

In this section, we study the scaling limit of the one and two-point correlation functions of the transverse magnetisation after a spin flip ($d_0 = 1$), $\mathcal{M}_t(j) = \langle \Psi(t) | \sigma_j^z | \Psi(t) \rangle$ and $\mathcal{M}_t(j, j') = \langle \Psi(t) | \sigma_j^z \sigma_{j'}^z | \Psi(t) \rangle$. The basis $|l_1 l_2\rangle$ appearing in the decomposition (7) of the state is particularly convenient, as it is an eigenbasis for the local transverse magnetisation operators,

$$\sigma_j^z |l_1 l_2\rangle = \text{sgn}(l_1 - j) \text{sgn}(l_2 - j) |l_1 l_2\rangle. \quad (14)$$

Said otherwise, in the state $|l_1 l_2\rangle$ the magnetisation is -1 between the two domain walls, and $+1$ otherwise. Since spins are associated to integer positions and domain walls to half-integer ones, there is no ambiguity in the above expression. Using that $\text{sgn } x = 2\theta(x) - 1$, and inserting Eq. (14) into the expression of the correlation functions, we can express both quantities in terms of the same operator:

$$\begin{cases} \mathcal{M}_t(j) = 1 - 2 \langle \Psi(t) | \Pi_{[-\infty, j-1/2]}^{[j+1/2, +\infty]} | \Psi(t) \rangle, \\ \mathcal{M}_t(j, j') = 1 - 2 \langle \Psi(t) | \Pi_{[j+1/2, j'-1/2]}^{[j'+1/2, +\infty]} + \Pi_{[-\infty, j-1/2]}^{[j+1/2, j'-1/2]} | \Psi(t) \rangle, \end{cases} \quad (15)$$

where

$$\Pi_X^Y = \sum_{\substack{l_1 \in X, l_2 \in Y \\ l_1 < l_2}} |l_1 l_2\rangle \langle l_1 l_2|. \quad (16)$$

Physically, for two sets of neighbouring half-integers $X = \llbracket x_l, x_r \rrbracket$ and $Y = \llbracket y_l, y_r \rrbracket$ the expectation value of the projector $p_{(X, Y)}(t) = \langle \Psi(t) | \Pi_X^Y | \Psi(t) \rangle$ gives the probability to find one domain wall in X and the other in Y at time t . We now proceed to define its scaling limit: we take $|x_l|, |x_r|, |y_l|, |y_r| \rightarrow \infty$ while keeping the ratios $x_{l,r}/t$ and $y_{l,r}/t$ (the rays) fixed, and maintaining a constant initial domain size $d_0 = 1$:

$$\underline{p}_{(\mathcal{X}, \mathcal{Y})} = \lim_{\substack{|x_{l,r}|, |y_{l,r}|, t \rightarrow \infty \\ (x_l/t, x_r/t) \rightarrow \mathcal{X} \\ (y_l/t, y_r/t) \rightarrow \mathcal{Y}}} p_{(X, Y)}(t). \quad (17)$$

In this expression, the discrete intervals $X = \llbracket x_l, x_r \rrbracket$ are associated to continuous ray intervals $\mathcal{X} = (x_l/t, x_r/t)$. As shown in appendix B, we can decompose the scaling limit (17) into a contribution coming from the scattering states $\langle \psi(t) | \Pi_X^Y | \psi(t) \rangle$ and one from the bound states $\langle \nu(t) | \Pi_X^Y | \nu(t) \rangle$ as $\underline{p}_{(\mathcal{X}, \mathcal{Y})} =$

$\underline{p}_{(\mathcal{X}, \mathcal{Y})}^S + \underline{p}_{(\mathcal{X}, \mathcal{Y})}^B$, where

$$\begin{cases} \underline{p}_{(\mathcal{X}, \mathcal{Y})}^S = \frac{1}{4\pi^2} \int_{-\pi}^{\pi} dk_1 dk_2 |\tilde{\psi}(k_1, k_2)|^2 \Theta[\epsilon'_{k_1} \in \mathcal{X}] \Theta[\epsilon'_{k_2} \in \mathcal{Y}] \theta(v_{k_2} - v_{k_1}), \text{ and} \\ \underline{p}_{(\mathcal{X}, \mathcal{Y})}^B = \frac{1}{2\pi} \int_{-\pi}^{\pi} dK (1 - e^{-2\eta(K)}) \Theta[E'_K \in \mathcal{X} \cap \mathcal{Y}] \theta(\Delta - |\cos \frac{K}{2}|). \end{cases} \quad (18)$$

In this expression we use the indicator function $\Theta[P]$ which evaluates to 1 if P is true and 0 otherwise. Here the latter can always be expressed as a product of Heaviside step functions.

The following limits have a very simple interpretation: the probability density for the positions of the scattering state corresponds to an interference pattern between two semi-classical trajectories $x_k(t) = \epsilon'_k t$. Indeed, recall that $|\psi(k_1, k_2)|^2 = |1 + S(k_1, k_2)e^{-i(k_1 - k_2)}|^2$. The first term corresponds to trajectories without crossing, whereas the second one corresponds to those with an exchange (and thus a crossing) of the two particles. In this second configuration the wavefunction acquires a phase $S(k_1, k_2)e^{-i(k_1 - k_2)}$.

In contrast, bound states become point-like in the scaling limit, following the semi-classical trajectory $x_K(t) = E'_K t$. Their contribution to the expectation value of the projector Π_X^Y stays non-zero in the scaling limit only if X and Y have a non-zero intersection.

The latter result can directly be used to compute the scaling limit of the one- and two-point function of the transverse magnetisation, which read

$$\begin{cases} \underline{\mathcal{M}}(\xi) = p^B + \int_{-\pi}^{\pi} \frac{dk_1 dk_2}{8\pi^2} |1 + S(k_1, k_2)e^{i(k_1 - k_2)}|^2 \operatorname{sgn}(v_{k_1} - \xi) \operatorname{sgn}(v_{k_2} - \xi) \text{ and} \\ \underline{\mathcal{M}}(\xi_1, \xi_2) = p^B + \int_{-\pi}^{\pi} \frac{dk_1 dk_2}{8\pi^2} |1 + S(k_1, k_2)e^{i(k_1 - k_2)}|^2 \operatorname{sgn}(v_{k_1} - \xi_1) \operatorname{sgn}(v_{k_2} - \xi_1) \operatorname{sgn}(v_{k_1} - \xi_2) \operatorname{sgn}(v_{k_2} - \xi_2). \end{cases} \quad (19)$$

From these formulas it is evident that the local perturbation leads to a macroscopic deformation of the magnetisation profile, as the latter is affected by an $\mathcal{O}(1)$ correction across the entire light-cone of size $\sim 2t$. An interesting aspect of interactions in this setting is that the non-locality of the elementary excitations amplifies quantum interferences to ballistic scales. Therefore, the scattering phase becomes essentially "readable" directly from the magnetisation profile. We can also see from the expression of the two-point function that it does not factorise into a product of one-point functions, even though two different ray variables ξ_1 and ξ_2 correspond to a physical distance $(\xi_1 - \xi_2)t$ that diverges linearly in time. Even though the initial state is a trivial product state, the perturbation thus induces a breaking of clustering properties. The most important way the interaction affects this picture is through the creation of bound states, which do not participate to the breaking of clustering. Indeed, as $\Delta \rightarrow \infty$ the probability p^B of forming a bound state gets higher and both the one and two-point scaling limits of the magnetisation tend to the uniform magnetisation of the ground state, $\underline{\mathcal{M}}(\xi_1, \xi_2) = \underline{\mathcal{M}}(\xi_1)\underline{\mathcal{M}}(\xi_2) = 1$.

In FIG 1, we compare this prediction with exact numerical data. The agreement is already excellent at early times, except in the region $(-\min(1, 1/(2\Delta)), \min(1, 1/(2\Delta)))$ corresponding to the light-cone of the bound state, where a $\mathcal{O}(t^{-1})$ correction becomes very visible as Δ increases. This disagreement is a finite time effect, since the finite width of the bound state becomes negligible as $t \rightarrow \infty$.

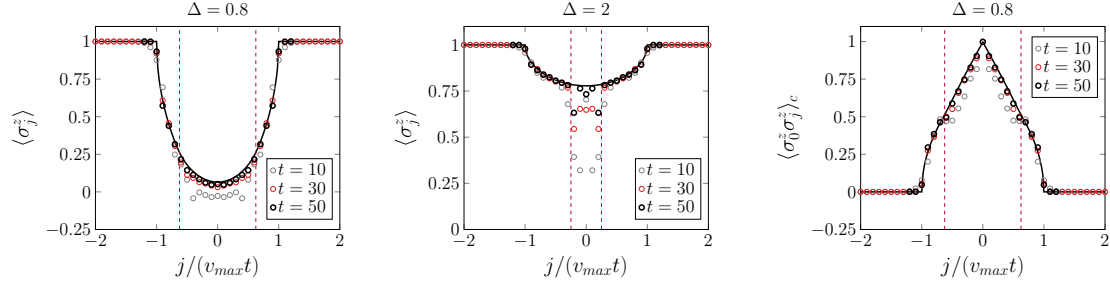


FIG. 1. Magnetisation profile and connected correlations after a spin flip at site $l = 0$ on the state $|\uparrow\rangle$ for different values of Δ . Points correspond to exact values of the magnetisation while the solid curve represents the asymptotic limit of Eq.(19). In the two rightmost plots the dashed line represent the maximal bound state velocity $v_{max}^B = \min(1, 1/(2\Delta))$.

V. SCALING LIMIT OF THE REDUCED DENSITY MATRIX

A. Exact RDM

In the rest of the paper, we aim to compute quantities that require the knowledge of the reduced density matrix for subsystems of neighbouring spins. We consider the subsystem $A = [\![l, r]\!]$, and also introduce the "dual subsystem" corresponding to domain wall positions, $\tilde{A} = [\![l - \frac{1}{2}, r + \frac{1}{2}]\!]$. The partial trace of $|l_1 l_2\rangle \langle m_1 m_2|$ is non-zero only if the domain wall configuration in \tilde{A}^c are identical for the bra and the ket:

$$\text{Tr}_{A^c}(|l_1 l_2\rangle \langle m_1 m_2|) = |l_1 l_2\rangle_A \langle m_1 m_2|_A t_{l_1 m_1}^A t_{l_2 m_2}^A. \quad (20)$$

Here, $|l_1 l_2\rangle_A$ represents the state in the subsystem A in presence of two domain walls at positions l_1 and l_2 :

$$|l_1 l_2\rangle_A = \bigotimes_{j \in A} (\Theta[j \in (l_1, l_2)] |\downarrow\rangle + \Theta[j \notin (l_1, l_2)] |\uparrow\rangle), \quad (21)$$

and the matrix t_{ij}^A enforces the domain walls outside A to match:

$$t_{ij}^A = \begin{cases} 1 & \text{if } i, j \in \tilde{A}, \\ \delta_{ij} & \text{otherwise.} \end{cases} \quad (22)$$

Using this formalism, we can explicitly write the RDM $\rho_A(t) = \text{Tr}_{A^c}(|\Psi(t)\rangle \langle \Psi(t)|)$. Dropping the explicit time dependence of the wavefunction and density matrix,

$$\rho_A = \text{Tr}_{A^c}(|\Psi\rangle \langle \Psi|) = \sum_{ij, kl \in \tilde{A}} \rho_{ij, kl}^A |ij\rangle_A \langle kl|_A + \left(1 - \sum_{i, j \in \tilde{A}} \rho_{ij, ij}^A\right) |\uparrow\rangle_A \langle \uparrow|_A, \quad (23)$$

where the first term captures the contributions that can be expressed as two domain walls in \tilde{A} :

$$\rho_{ij, kl}^A = \sum_{l_1 l_2 m_1 m_2} \Psi_{l_1 l_2} \Psi_{m_1 m_2} t_{l_1 m_1}^A t_{l_2 m_2}^A \langle l_1 l_2 |ij\rangle_A \langle kl | m_1 m_2 \rangle_A, \quad (24)$$

and the remaining terms are collected in the vacuum term $|\uparrow\rangle\langle\uparrow|$, corresponding to configurations where both domain walls are outside of the subsystem and on the same side.

B. Scaling limit

In the scaling limit $|l|, |r|, t \rightarrow \infty$ with l/t and r/t fixed, the RDM admits a simplified structure in the sense that both its eigenvalues and the matrix elements of products of odd operators between its eigenvectors admit a scaling limit.

In order to see this, we separate the domain wall positions between three regions: $\tilde{A} = [\![l - \frac{1}{2}, r + \frac{1}{2}]\!]$, the left complement $\tilde{L} = [-\infty, l - \frac{3}{2}]\!$, and the right complement $\tilde{R} = [r + \frac{3}{2}, +\infty]\!$. Since t_{ij}^A , controlling the partial trace, is block-diagonal between these three regions, the RDM naturally decomposes between contributions (X, Y) representing the positions of the two domain walls:

$$\rho_A = \sum_{X, Y \in \{\tilde{L}, \tilde{A}, \tilde{R}\}} p_{(X, Y)} \rho_{A(X, Y)}, \quad (25)$$

where $p_{(X, Y)}$ is the probability to find a domain wall in X and the other in Y , see Eq. (18), and the density matrix associated to this configuration is defined as:

$$p_{(X, Y)} \rho_{A(X, Y)} = \text{Tr}_{A^c} (\Pi_X^Y |\Psi\rangle\langle\Psi| \Pi_X^Y). \quad (26)$$

Technically, $\rho_{A(\tilde{L}, \tilde{R})}, \rho_{A(\tilde{L}, \tilde{A})}, \rho_{A(\tilde{A}, \tilde{R})}$ and $\rho_{A(\tilde{A}, \tilde{A})}$ share the boundary state $|l - \frac{1}{2}, r + \frac{1}{2}\rangle_A$, but this overlap becomes irrelevant in the scaling limit. Therefore, we ignore this subtlety and refer to $\rho_{A(\tilde{L}, \tilde{R})} + \rho_{A(\tilde{L}, \tilde{A})} + \rho_{A(\tilde{A}, \tilde{R})}$ as the 0-particle sector, $\rho_{A(\tilde{L}, \tilde{A})} + \rho_{A(\tilde{A}, \tilde{R})}$ as the 1-particle sector and $\rho_{A(\tilde{A}, \tilde{A})}$ as the 2-particle sector.

1. Pure and trivial sectors

Several sectors simplify immediately: the 0-particle sector simply corresponds to a statistical mixture of the two SSB vacua. If both domain walls belong to the same complement, A is in the same vacuum as the initial state before the perturbation. If instead they are on both sides of A the latter is effectively "flipped":

$$\rho_{A(\tilde{L}, \tilde{L})} = \rho_{A(\tilde{R}, \tilde{R})} = |\uparrow\rangle_A\langle\uparrow|_A \quad \text{and} \quad \rho_{A(\tilde{L}, \tilde{R})} = |\downarrow\rangle_A\langle\downarrow|_A. \quad (27)$$

Furthermore, the 2-particle sector remains pure after taking the partial trace:

$$\rho_{A(\tilde{A}, \tilde{A})} = p_{(\tilde{A}, \tilde{A})} |\Psi_A\rangle\langle\Psi_A|, \quad \text{with} \quad |\Psi_A\rangle = \frac{1}{\sqrt{p_{(\tilde{A}, \tilde{A})}}} \sum_{l_1 < l_2 \in \tilde{A}} \Psi_{l_1, l_2} |l_1 l_2\rangle_A. \quad (28)$$

For any internal regions $X, Y \subset A$, $\langle\Psi_A|\Pi_X^Y|\Psi_A\rangle$ is given by the probability ratio

$$\langle\Psi_A|\Pi_X^Y|\Psi_A\rangle = \frac{p_{(X, Y)}}{p_{(A, A)}}, \quad (29)$$

which ensures that the expectation value of any product of local odd operators in $|\Psi_A\rangle$ admits a scaling limit.

2. Diagonalisation of the 1-particle sector

Complications arise from the terms $\rho_{A(\tilde{L}, \tilde{A})}$ and $\rho_{A(\tilde{A}, \tilde{R})}$, that have a more complex structure:

$$\rho_{A(\tilde{L}, \tilde{A})} \simeq \sum_{\substack{l_1 \in \tilde{L} \\ l_2, m_2 \in \tilde{A}}} \psi_{l_1, l_2} \psi_{l_1 m_2}^* |l_2\rangle_A \langle m_2|_A \quad (30)$$

$$\rho_{A(\tilde{A}, \tilde{R})} \simeq \sum_{\substack{l_1, m_1 \in \tilde{A} \\ l_2 \in \tilde{R}}} \psi_{l_1 l_2} \psi_{m_1 l_2}^* P_A |l_1\rangle_A \langle m_1|_A P_A, \quad (31)$$

where we define $|m\rangle_A = |l - \frac{1}{2}, m\rangle_A$, $P_A |m\rangle_A = |m, r + \frac{1}{2}\rangle_A$. In this expression ψ_{l_1, l_2} is the scattering states wavefunction, see Eq. (8). We dropped the bound states contribution that vanishes in the scaling limit (see Eq. (18)) since \tilde{L} , \tilde{A} and \tilde{R} have no overlap. The effective number of terms in the sum over \tilde{L} (resp. \tilde{R}) diverges linearly in time as the light-cone expands. On the other hand, each individual term vanishes like $1/t$, making the scaling non-obvious. To resolve this issue, we recall the integral representation of $\psi_{l_1 l_2}$:

$$\psi_{f_1, f_2} = \frac{1}{4\pi^2} \int_{-\pi}^{\pi} dk_1 dk_2 \tilde{\psi}(k_1, k_2) e^{i[k_1(f_1-1/2) + k_2(f_2+1/2)]} e^{-i(\epsilon_{k_1} + \epsilon_{k_2})t}. \quad (32)$$

The coupling between the two domain walls is entirely contained within the function $\tilde{\psi}_{d_0}(k_1, k_2) = e^{i(k_1 - k_2)} + S(k_1, k_2)$. Since the scattering phase satisfies $S(k_1, k_2) = S(k_2, k_1)^*$, it can be seen as the Kernel of a Hermitian operator acting on the compact support $(-\pi, \pi)$. By the Hilbert-Schmidt theorem, it can be decomposed as

$$S(k_1, k_2) = \sum_{j=1}^{+\infty} \lambda_j \phi_j(k_1) \phi_j^*(k_2), \quad (33)$$

where the set of eigenvalues λ_j is discrete, accumulating only around 0 and the eigenfunctions ϕ_j are orthonormal: $\int_{-\pi}^{\pi} dk \phi_j(k) \phi_{j'}^*(k) = 2\pi \delta_{jj'}$. The dominant terms of Eq. (33) can be very well approximated numerically by diagonalising the truncated matrix of Fourier coefficients of $S(k_1, k_2)$, given in appendix D. The properties of the scattering phase,

$$S(k, k) = -1 \text{ and } S(k_1, k_2) S(k_2, k_1) = 1, \quad (34)$$

impose the eigenvalues to satisfy

$$\sum_{j=1}^{+\infty} \lambda_j = -1 \text{ and } \sum_{j=1}^{+\infty} \lambda_j^2 = 1. \quad (35)$$

These identities provide a robust consistency check of the numerical diagonalisation. To recover the full expression of $\psi_{d_0}(k_1, k_2)$, we define $\lambda_0 = 1$ and $\phi_0(k) = e^{i d_0 k}$ in such a way that $\psi_{d_0}(k_1, k_2) = \sum_{j=0}^{+\infty} \lambda_j \phi_j(k_1) \phi_j^*(k_2)$. Furthermore, we introduce the \tilde{X} -restricted Gram matrices of the modes ϕ_j as:

$$G_{jj'}(\tilde{X}) = \sum_{l \in \tilde{X}} \left(\frac{1}{4\pi^2} \int_{-\pi}^{\pi} dk dp \phi_j(k) \phi_{j'}^*(p) e^{i(k-p)(l-1/2)} e^{-i(\epsilon_k - \epsilon_p)t} \right) \quad (36)$$

$$G_{jj'}^c(\tilde{X}) = \sum_{l \in \tilde{X}} \left(\frac{1}{4\pi^2} \int_{-\pi}^{\pi} dk dp \phi_{j'}^*(k) \phi_j(p) e^{i(k-p)(l+1/2)} e^{-i(\epsilon_k - \epsilon_p)t} \right). \quad (37)$$

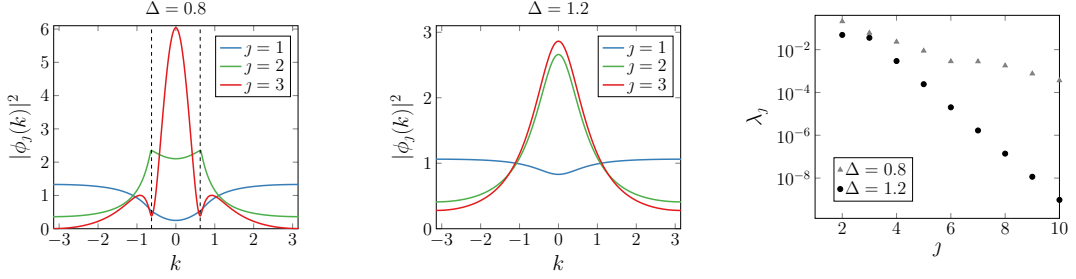


FIG. 2. Numerical diagonalisation of the scattering phase using its truncated Fourier representation S_{nm} with $|n|, |m| \leq 250$. For $\Delta = 0.8$, $\sum_j \lambda_j \approx 0.996611$ and $\sum_j \lambda_j^2 \approx 0.999991$, while for $\Delta = 1.2$ $\sum_j \lambda_j \approx 1$ and $\sum_j \lambda_j^2 \approx 0.1$ up to at least 10^{-8} precision. Left and center: representation of the first modes of the scattering phase. The dashed lines represent the momenta $\pm \cos^{-1} \Delta$ at which the scattering phase becomes non-analytic. Right: eigenvalues of the truncated Fourier representation of the scattering phase.

These definitions allow to recast Eq. (30) as a discrete sum over the eigenvalues λ_j , which typically decay exponentially, see Fig 2. If we focus on $\rho_{A(\tilde{L}, \tilde{A})}$, we get

$$\rho_{A(\tilde{L}, \tilde{A})} = \sum_{j, j'=0}^{+\infty} \lambda_j \lambda_{j'} G_{jj'}(\tilde{L}) |\phi_{j'}\rangle_A \langle \phi_j|_A. \quad (38)$$

The states $|\phi_j\rangle_A$ are the lattice representation of the eigenfunction $\phi_j(k)$ on the subsystem A :

$$|\phi_j\rangle_A = \sum_{l \in \tilde{A}} \frac{1}{2\pi} \int_{-\pi}^{\pi} dk \phi_j^*(k) e^{ik(l-1/2)} e^{-i\epsilon_k t} |l\rangle_A, \quad \langle \phi_j | \phi_{j'} \rangle_A = G_{jj'}^c(\tilde{A}). \quad (39)$$

This framework reduces the problem of finding the eigenvectors and eigenvalues of ρ_A to that of diagonalising the matrix $M^{(\tilde{L}, \tilde{A})} = \Lambda G(\tilde{L}) \Lambda(G^c(\tilde{A}))$, where $\Lambda = \text{diag}(\{\lambda_j\})$. In the scaling limit, the Gram matrices $G(\tilde{X})$ and $G^c(\tilde{X})$ converge to the overlap of the eigenfunctions $\phi_j(k)$ restricted to the ray-interval \mathcal{X} :

$$\underline{G}_{jj'}(\mathcal{X}) = (\underline{G}_{j'j}^c(\mathcal{X}))^* = \frac{1}{2\pi} \int_{-\pi}^{\pi} dk \phi_j(k) \phi_{j'}^*(k) \Theta[\epsilon'_k \in \mathcal{X}]. \quad (40)$$

The existence of this limit ensures that the spectrum of $\rho_{A(\tilde{L}, \tilde{A})}$ admits a well-defined scaling limit, namely:

$$\{\underline{\mu}_j^{A(\mathcal{L}, \mathcal{A})}\} = \text{Spec}[\Lambda \underline{G}(\mathcal{L}) \Lambda \underline{G}^\dagger(\mathcal{A})]. \quad (41)$$

Furthermore, the eigenvectors of $\rho_{A(\tilde{L}, \tilde{A})}$ are given by a linear combination of the states $|\phi_{j'}\rangle_A$,

$$|\varphi_n^{A(\tilde{L}, \tilde{A})}\rangle = \sum_j W_{nj}^{(\tilde{L}, \tilde{A})} |\phi_j\rangle_A, \quad (42)$$

where the coefficients $W_{nj}^{(\tilde{L}, \tilde{A})}$ are the eigenvectors of $M^{(\tilde{L}, \tilde{A})}$. These coefficients converge to stable values $\underline{W}_{nj}^{(\mathcal{L}, \mathcal{A})}$ in the scaling limit, namely the eigenvectors of $\underline{M}^{(\mathcal{L}, \mathcal{A})} = \Lambda \underline{G}(\mathcal{L}) \Lambda \underline{G}^\dagger(\mathcal{A})$.

VI. ENTANGLEMENT ASYMMETRY

Having access to the details of the reduced density matrix ρ_A for a subsystem of neighbouring spins A , we now proceed to study the nature of the transverse magnetisation correlations within A . Introducing the total transverse magnetisation within the subsystem, $Z_A = \sum_{j \in A} \sigma_j^z$, we first focus on the entanglement asymmetry of ρ_A with respect to Z_A :

$$\Delta S(\rho_A, Z_A) = S(\mathcal{G}_{Z_A}(\rho_A)) - S(\rho_A). \quad (43)$$

This quantity is defined as the relative entropy between the state ρ_A and its “twirled” version,

$$\mathcal{G}_{Z_A}(\rho_A) = \sum_{z \in \text{Spec } Z_A} \Pi_z \rho_A \Pi_z. \quad (44)$$

It is expressed in terms of the projector Π_z on the eigenspace of Z_A with eigenvalue z . The twirled state $\mathcal{G}_{Z_A}(\rho_A)$ represents the state of A after a non-selective measurement of Z_A : physically, this operation removes all off-diagonal elements - corresponding to coherence - between charge sectors. Consequently, while the fluctuations of Z_A in ρ_A and $\mathcal{G}_{Z_A}(\rho_A)$ are identical, those in the twirled state can be interpreted as solely due to classical uncertainty.

$\Delta S(\rho_A, Z_A)$ is an asymmetry measure with respect to the $U(1)$ group generated by Z_A . While the latter is not a symmetry of the Hamiltonian, it is a symmetry of the SSB ground state, which has fixed magnetisation. The Entanglement Asymmetry (EA) satisfies two important properties: (i) it is positive [81], $\Delta S(\rho_A, Z_A) \geq 0$, and (ii) it vanishes precisely when the state is symmetric with respect to the charge [34], i.e., when there is no coherence between charge sectors,

$$\Delta S(\rho_A, Z_A) = 0 \Leftrightarrow [\rho_A, Z_A] = 0.$$

After a local quench on the SSB ground state, one can expect the symmetry to be violated at intermediate times as excitations propagate, and then restored at late times as the system locally relaxes into the zero-particle sector.

Computing the exact value of ΔS_Z is generally a formidable task. However, in our setting, we can take advantage of the low dimensionality of the 2-particle sector to numerically compute its exact value in a time that scales polynomially with respect to the subsystem size.

To gain physical insight into the behaviour of $\Delta S(\rho_A, Z_A)$, we note that its leading behaviour is relatively insensitive to the structure of the RDM. Actually, we can work out two simple bounds to approximate it. Let B be the complement of region A , and let us define the twirled state of pure system $|\Psi\rangle$ with respect to Z_A :

$$\sigma^{(A)} = \mathcal{G}_{Z_A}(|\Psi\rangle\langle\Psi|). \quad (45)$$

Since the twirling operator acts non-trivially only on the subsystem A , it satisfies

$$\text{Tr}_B(\sigma^{(A)}) = \mathcal{G}_{Z_A}(\text{Tr}_B(|\Psi\rangle\langle\Psi|)) = \mathcal{G}_{Z_A}(\rho_A), \quad (46)$$

$$\text{Tr}_A(\sigma^{(A)}) = \text{Tr}_A \left(\sum_{z \in \text{Spec } Z_A} \Pi_z |\Psi\rangle\langle\Psi| \Pi_z \right) = \text{Tr}_A(|\Psi\rangle\langle\Psi|) = \rho_B. \quad (47)$$

The triangle inequality for entanglement entropy $S_{AB} \geq |S_A - S_B|$ applied to $\sigma^{(A)}$ yields

$$S(\sigma^{(A)}) \geq |S(\mathcal{G}_{Z_A}(\rho_A)) - S(\rho_B)|. \quad (48)$$

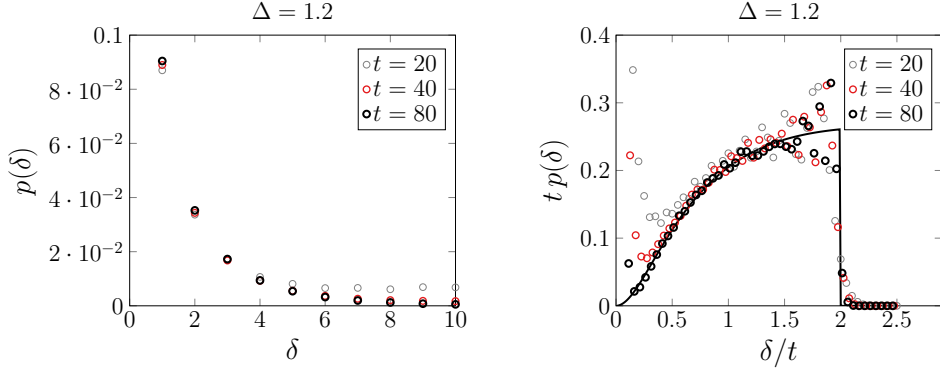


FIG. 3. Probability $p(\delta)$ to find two domain walls separated by a distance δ . Left: time-independent contribution to the probability distribution (bound states). Right: scaling limit of the time-dependent part of the distribution (scattering states). The numerical data is compared with the (coarsened grained) underlying continuous distribution.

Recalling that $|\Psi\rangle\langle\Psi|$ is pure, $S(\rho_A) = S(\rho_B)$. Therefore, the inequality becomes:

$$S(\sigma^{(A)}) \geq \Delta S(\rho_A, Z_A). \quad (49)$$

Note that the entropy of $\sigma^{(A)}$ is precisely the asymmetry of the full state with respect to Z_A , since $S(|\Psi\rangle\langle\Psi|) = 0$. On the other hand, the subadditivity of the Von-Neumann entropy, $S(\rho_{AB}) \leq S(\rho_A) + S(\rho_B)$, applied to $\sigma^{(A)}$ gives a lower bound:

$$S(\sigma^{(A)}) \leq S(\mathcal{G}_{Z_A}(\rho_A)) + S(\rho_B). \quad (50)$$

Rearranging and substituting $S(\rho_A) = S(\rho_B)$, we finally obtain that the subsystem asymmetry is bounded by the entropy of the charge fluctuations:

$$S(\sigma^{(A)}) - 2S(\rho_A) \leq \Delta S(\rho_A, Z_A) \leq S(\sigma^{(A)}). \quad (51)$$

Our analysis in section V implies that the entanglement entropy $S(\rho_A)$ admits a well-defined scaling limit, given by the Shannon entropy of the RDM eigenvalues $\underline{\mu}_j^A$:

$$S(\rho_A) \rightarrow - \sum_j \underline{\mu}_j^A \log \underline{\mu}_j^A. \quad (52)$$

The eigenvalues $\underline{\mu}_j^A$ decay rapidly (a consequence of the decay of the Hilbert-Schmidt coefficients λ_j), so this limit is finite. Consequently, the entanglement entropy $S(\rho_A)$ contributes only an $\mathcal{O}(1)$ term to the total asymmetry. In the scaling limit, we can therefore approximate the entanglement asymmetry using the asymmetry $S(\sigma^{(A)})$ of the full state $|\Psi\rangle$ with respect to the subsystem charge Z_A :

$$\Delta S(\rho_A, Z_A) = S(\sigma^{(A)}) + \mathcal{O}(1). \quad (53)$$

This approximation is particularly useful because $S(\sigma^{(A)})$ only depends on the probability distribution $p_{Z_A}(z)$ for the different possible magnetisations in A :

$$S(\sigma^{(A)}) = - \sum_{z \in \text{Spec}(Z_A)} p_{Z_A}(z) \log p_{Z_A}(z), \quad (54)$$

which is much easier to compute than the exact entanglement asymmetry of ρ_A . The probability of finding a magnetisation $Z_A = |A| - 2d$ (corresponding to d flipped spins) is given by

$$\begin{aligned} p_{Z_A}(|A| - 2d) &= \delta_{d,0}(p_{(\tilde{L},\tilde{L})} + p_{(\tilde{R},\tilde{R})}) + \delta_{d,|A|}(p_{(\tilde{L},\tilde{R})}) \\ &+ \sum_{j \leq l - \frac{1}{2}} |\Psi_{j,l-\frac{1}{2}+d}|^2 + \sum_{j' \geq r + \frac{1}{2}} |\Psi_{r+\frac{1}{2}-d,j'}|^2 + \sum_{j=l+\frac{1}{2}}^{r-\frac{1}{2}-d} |\Psi_{j,j+d}|^2. \end{aligned} \quad (55)$$

The extreme values of the magnetisation, $Z_A = \pm|A|$, carry an $\mathcal{O}(1)$ weight corresponding to the configurations where both domain walls are outside the subsystem. Similarly, the bound states give $\mathcal{O}(1)$ contributions to the near-to-maximal magnetisations, $Z_A = |A| - 2d$, that decay exponentially with d .

In contrast, the scattering states give $\mathcal{O}(1/t)$ contributions spread on a support of size $\sim 2t$ (the size of the light-cone) when at least one domain wall is inside the subsystem. This distinction has a strong impact on the behaviour of the asymmetry for different Rényi indexes α . For $\alpha > 1$, the sum is dominated by the $\mathcal{O}(1)$ weights (vacuum and bound states), while the Von-Neumann ($\alpha = 1$) asymmetry is dominated by the $\mathcal{O}(1/t)$ contributions. Consequently, the standard Replica trick [82, 83] methods to compute the limits as $n \rightarrow 1$ of $\text{Tr}(\rho_A^n)$ and $\text{Tr}(\mathcal{G}_{Z_A}(\rho_A)^n)$ are not adapted to this problem. Keeping only the dominant $\mathcal{O}(1/t)$ terms, we find that the asymmetry should behave as

$$\Delta S(\rho_A, Z_A) = (p^S - p_0^S(t)) \log(2t) + \mathcal{O}(1), \quad (56)$$

where $p_0^S(t) = p_{(\tilde{L},\tilde{L})}^S(t) + p_{(\tilde{R},\tilde{R})}^S(t) + p_{(\tilde{L},\tilde{R})}^S(t)$ is the time-dependant probability to have a scattering state where both domain walls are outside the subsystem. This formula implies that the quantity $\Delta S(\rho_A, Z_A)/\log(2t)$ is well defined in the scaling limit:

$$\lim_{\substack{|A|, t \rightarrow \infty \\ t/|A| = \tau}} \frac{\Delta S(\rho_A, Z_A)}{\log(2t)} = p^S - \underline{p}_0^S(\tau). \quad (57)$$

The logarithmic growth is a consequence of the ballistic spreading of the domain walls, resulting in the state coherently spanning a number of magnetisation sectors that diverges in time. At late times $t \gg |A|$, the probability $p_0^S(t)$ approaches p^S as $1/t$ as the slowest quasiparticles escape the subsystem. Consequently, the asymmetry vanishes to its vacuum value as the symmetry is locally restored. The leading behaviour of the asymmetry is quite universal, and is affected by interactions only through the term $p^S - \underline{p}_0^S(t)$ that discards the bound states.

While Eq. (57) captures the leading-term behaviour of the asymmetry, in practice the $\mathcal{O}(1)$ correction is comparable with the logarithmic one for the times and subsystem sizes we study numerically. At intermediate times $t < |A|/2$, the subsystem is effectively pure as the quasiparticles from the initial perturbation have not yet reached the subsystem boundaries. In this regime the $\mathcal{O}(1)$ correction can be very well approximated by a constant term ΔS_0 , taking into account the contribution of the bound state (see left panel of Fig. 3) and the differential entropy associated with the non-oscillating part of the probability distribution for the magnetisation (right panel of Fig. 3). Taking into account this correction allows for a very good fit of the

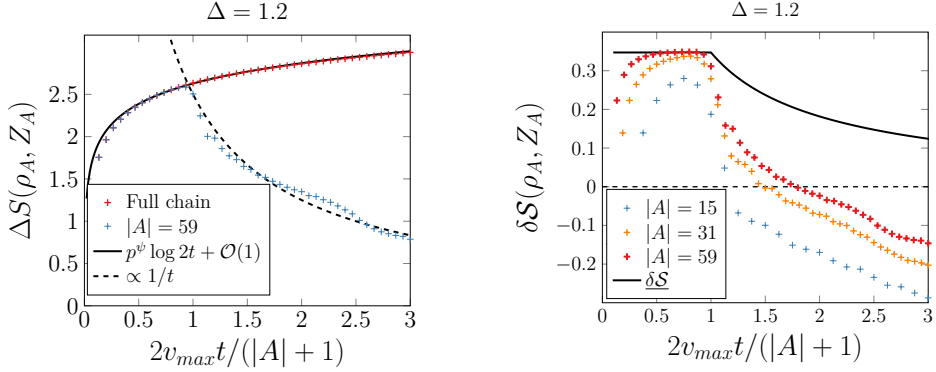


FIG. 4. Left: Time evolution of asymmetry after a spin flip. Right: Comparison between the asymptotic prediction and the numerical values of $\delta\mathcal{S}(\rho_A, Z_A) = (\Delta S(\rho_A, Z_A) - \Delta S_0) / \log t$ for different subsystem sizes.

numerical data, see Fig 4. Conversely, both the bound state and scattering states contributions to the non-vacuum part of the RDM can be expanded at late times as corrections to the infinite time (vacuum) limit. The probability to find a domain wall or a bound state in A decays as $1/t$, which preserves the predicted $1/t$ power-law decay of the asymmetry.

VII. QUANTUM FISHER INFORMATION

The entanglement asymmetry, discussed in the previous section, provides a rigorous measure of the coherence between the different magnetisation sectors. However, it effectively "counts" this number of sectors independently of the magnetisation associated to each of them. To further characterise the quantum fluctuations associated to coherence between different magnetisation sectors, it is natural to extend this study to the computation of the Quantum Fisher Information (QFI), which is sensitive to the magnitude of the fluctuations between the magnetisation sectors. We will actually work with the rescaled Quantum Fisher Information (rQFI) [24], which is defined for a density matrix $\rho = \sum_i \mu_i |i\rangle \langle i|$ and an observable O as

$$\chi(\rho, O) = \frac{1}{4||O||^2} \sum_{k,l=1}^{+\infty} \frac{(\mu_i - \mu_j)^2}{\mu_i + \mu_j} |\langle i | O | j \rangle|^2. \quad (58)$$

The reason we are specifically interested in the rQFI is its ability to detect the physical scale of quantum correlations, and in particular the breaking of clustering due to quantum superposition. To formalise this, we rely on the following properties of the rQFI:

a. *Link with variance:* For a pure state the QFI reduces to 4 times the variance, equivalently

$$\chi(|\psi\rangle \langle \psi|, O) = \frac{\text{Var}(|\psi\rangle \langle \psi|, O)}{||O||^2}. \quad (59)$$

b. *Sensitivity to pure coherence:* unlike the variance, the (r)QFI is convex:

$$\chi\left(\sum_i p_i \rho_i\right) \leq \sum_i p_i \chi(\rho_i), \quad (60)$$

and can actually be identified (up to a constant factor) with the convex roof of the variance [84]. This property ensures that, while the variance is sensitive to both classical and quantum fluctuations of O , the (r)QFI is only sensitive to quantum ones.

c. *Normalisation:* rQFI satisfies the bounds

$$0 \leq \chi(\rho, O) \leq 1. \quad (61)$$

While $\chi(\rho, O) = 0$ for a symmetric state ($[\rho, O] = 0$), it only attains its maximal value 1 for a cat-like state, i.e. an equal-weight superposition of two states with minimal ($\|O\|$) and maximal ($\|O\|$) values of O .

For these reasons, rQFI is able to detect a breakdown of clustering properties due to quantum superposition. In states with clustering, connected correlation functions $\langle o_i o_j \rangle_c = \langle o_i o_j \rangle - \langle o_i \rangle \langle o_j \rangle$ tend to 0 as the distance $|i - j|$ increases. In this setting, even in the presence of algebraically decaying correlations the variance of an extensive operator $\text{Var}(\rho_A, O_A)$ scales like some power of its volume, $|A|^\alpha$ with $\alpha < 2$. This implies

$$\chi(\rho_A, O_A) \leq \frac{\text{Var}(\rho_A, O_A)}{\|O_A\|^2} \underset{|A| \rightarrow \infty}{\rightarrow} 0. \quad (62)$$

Consequently, a non-zero value of χ in the scaling limit signals a violation of clustering at ballistic scales: the state must be a coherent superposition of magnetisation sectors whose total charges differ by an amount proportional to the system size. This effect was notably observed after a local quench on the SSB ground state of the Ising model in the ferromagnetic phase [24], or after joining a SSB ground state with a thermal one in the growing interface between order and disorder [22, 23]. This section aims to generalise the results of Ref. [24] to the interacting case and to introduce a Bethe-Ansatz method for computing the rQFI after local quenches.

Let $\underline{\chi}_{\mathcal{A}}$ be the value of the rescaled QFI in the limit $|A|, t \rightarrow \infty$ with the ratio $\tau = 2t/|A|$ held constant (we will see that such a limit exists). Taking advantage of decomposition (25) of the RDM: $\rho_A = \sum_{(X,Y)} p_{(X,Y)} \rho_{A(X,Y)}$, and noting that the magnetisation operator Z_A does not mix the different sectors (\tilde{X}, \tilde{Y}) in the scaling limit, the rQFI can be decomposed into the sum of the contributions from each sector of the RDM:

$$\underline{\chi}_{\mathcal{A}} = \sum_{(\mathcal{X}, \mathcal{Y})} p_{(\mathcal{X}, \mathcal{Y})} \underline{\chi}_{\mathcal{A}(\mathcal{X}, \mathcal{Y})}. \quad (63)$$

Here, $\underline{\chi}_{\mathcal{A}(\mathcal{X}, \mathcal{Y})}$ represents the scaling limit of the rQFI for the density matrix $\rho_{A(X,Y)}$. Since the sectors $(\mathcal{L}, \mathcal{L})$, $(\mathcal{R}, \mathcal{R})$, and $(\mathcal{L}, \mathcal{R})$ correspond to vacuum states, their contributions to the QFI are identically 0 (the variance of Z_A vanishes). The $(\mathcal{A}, \mathcal{A})$ sector - where both domain walls are inside the subsystem - is pure, therefore its contribution to the QFI is simply given by a variance. The calculation is done easily by integrating the scaling limit of $\langle \Psi_A | \sigma_i^z \sigma_j^z | \Psi_A \rangle_c$, given by Eq. (29). The result takes the simple form:

$$\begin{aligned} \underline{\chi}_{\mathcal{A}(\mathcal{A}, \mathcal{A})} &= \frac{4 \int_{-\pi}^{\pi} \frac{dk_1 dk_2}{8\pi^2} |\tilde{\psi}(k_1, k_2)|^2 (\epsilon'_{k_1} - \epsilon'_{k_2})^2 \Theta[\epsilon'_{k_1} \in \mathcal{A}] \Theta[\epsilon'_{k_2} \in \mathcal{A}]}{p_{(\mathcal{A}, \mathcal{A})}} \\ &\quad - \left(\frac{2 \int_{-\pi}^{\pi} \frac{dk_1 dk_2}{8\pi^2} |\tilde{\psi}(k_1, k_2)|^2 |\epsilon'_{k_1} - \epsilon'_{k_2}| \Theta[\epsilon'_{k_1} \in \mathcal{A}] \Theta[\epsilon'_{k_2} \in \mathcal{A}]}{p_{(\mathcal{A}, \mathcal{A})}} \right)^2. \end{aligned} \quad (64)$$

The sectors $(\mathcal{L}, \mathcal{A})$ and $(\mathcal{A}, \mathcal{R})$, where one domain wall is traced out, present the main difficulty as they are mixed states. However, numerical observation reveal that these sectors are almost pure. Therefore, the

rQFI is well approximated by the variance of Z_A in these states, with a rigorous bound given by the purity:

$$\frac{\text{Var}(\rho, \mathcal{O})}{\|\mathcal{O}\|^2} - 8 \left(1 - \sqrt{\text{Tr} \rho^2}\right) \leq \chi(\rho, \mathcal{O}) \leq \frac{\text{Var}(\rho, \mathcal{O})}{\|\mathcal{O}\|^2}, \quad (65)$$

that we derive in appendix C. Under this "pure state approximation", the $(\mathcal{L}, \mathcal{A})$ contribution to the rQFI simplifies to

$$\begin{aligned} \underline{\chi}_{\mathcal{A}(\mathcal{L}, \mathcal{A})}^{(\text{pure})} &= \frac{4 \int_{-\pi}^{\pi} \frac{dk_1 dk_2}{4\pi^2} |\tilde{\psi}(k_1, k_2)|^2 (\epsilon'_{k_2})^2 \Theta[\epsilon'_{k_1} \in \mathcal{L}] \Theta[\epsilon'_{k_2} \in \mathcal{A}]}{p_{(\mathcal{L}, \mathcal{A})}} \\ &\quad - \left(\frac{2 \int_{-\pi}^{\pi} \frac{dk_1 dk_2}{4\pi^2} |\tilde{\psi}(k_1, k_2)|^2 \epsilon'_{k_2} \Theta[\epsilon'_{k_1} \in \mathcal{L}] \Theta[\epsilon'_{k_2} \in \mathcal{A}]}{p_{(\mathcal{L}, \mathcal{A})}} \right)^2. \end{aligned} \quad (66)$$

Higher-order corrections to the rQFI

To go beyond this approximation, we assume that the eigenvalues $\mu_j^{A(\tilde{L}, \tilde{A})}$ of $\rho_{A(\tilde{L}, \tilde{A})}$ are indexed in such a way that they decrease with j . We then introduce the truncated reduced density matrix

$$\rho_{A(\tilde{L}, \tilde{A})}^{(n)} = \sum_{j=1}^n \mu_j^{A(\tilde{L}, \tilde{A})} |\varphi_j^{A(\tilde{L}, \tilde{A})}\rangle \langle \varphi_j^{A(\tilde{L}, \tilde{A})}|, \quad (67)$$

that only keeps the n dominant eigenvectors of the RDM. The advantage of using the truncated RDM is that using the techniques introduced in Section V, its rQFI $\underline{\chi}_{\mathcal{A}(\tilde{L}, \tilde{A})}^{(n)}$ in the scaling limit can be expressed as a finite sum involving the matrix elements $\underline{\mathcal{Z}}^{[1]}$ and $\underline{\mathcal{Z}}^{[2]}$ (the first and second moments of the velocity) over the n largest eigenvalues of the RDM:

$$\underline{\chi}_{\mathcal{A}(\mathcal{L}, \mathcal{A})}^{(n)} = \sum_{j=1}^n \underline{\mu}_j^{A(\mathcal{L}, \mathcal{A})} |\underline{\mathcal{Z}}_{jj}^{[2]\mathcal{A}(\mathcal{L}, \mathcal{A})}|^2 - 4 \sum_{i,j=1}^n \frac{\underline{\mu}_i^{A(\mathcal{L}, \mathcal{A})} \underline{\mu}_j^{A(\mathcal{L}, \mathcal{A})}}{\underline{\mu}_i^{A(\mathcal{L}, \mathcal{A})} + \underline{\mu}_j^{A(\mathcal{L}, \mathcal{A})}} |\underline{\mathcal{Z}}_{ij}^{[1]\mathcal{A}(\mathcal{L}, \mathcal{A})}|^2, \quad (68)$$

with (see Eq.(42))

$$\underline{\mathcal{Z}}_{mn}^{[\alpha]\mathcal{A}(\mathcal{L}, \mathcal{A})} = \sum_{i,j} (\underline{W}_{ni}^{(\mathcal{L}, \mathcal{A})})^* \underline{W}_{mj}^{(\mathcal{L}, \mathcal{A})} \int_{-\pi}^{\pi} \frac{dk}{2\pi} \phi_i^*(k) \phi_j(k) (2\epsilon'_k)^\alpha \Theta[\epsilon'_k \in \mathcal{A}]. \quad (69)$$

In appendix C, we also derive the following bounds for the rQFI of the truncated RDM, which ensures that the exact QFI can be approached to any level of precision simply by increasing n :

$$\underline{\chi}_{\mathcal{A}(\tilde{L}, \tilde{A})}^{(n)} - 4n\underline{\epsilon}_n \leq \underline{\chi}_{\mathcal{A}(\tilde{L}, \tilde{A})} \leq \underline{\chi}_{\mathcal{A}(\tilde{L}, \tilde{A})}^{(n)} + \underline{\epsilon}_n, \quad (70)$$

where $\underline{\epsilon}_n = \sum_{j=n+1}^{+\infty} \underline{\mu}_j^{A(\mathcal{L}, \mathcal{A})}$ is the missing weight in the truncated RDM.

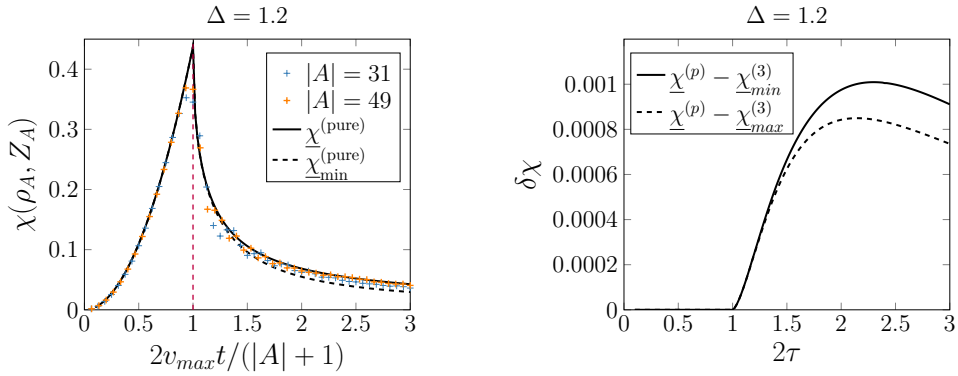


FIG. 5. Left: time evolution of the rQFI for two subsystems of lengths $|A| = 31$ and $|A| = 49$ centered around the initial spin flip, compared with the analytical bounds for the rQFI in the scaling limit, see Eq. (65). Right: higher-order corrections to the rQFI, see Eq. (68), (69) and (70).

Discussion

In the left panel of Fig. 5, we compare the prediction of the "pure approximation" with exact numerical data, together with the predicted lower bound which is obtained directly from the eigenvalues of $\rho_{A(\tilde{L}, \tilde{A})}$ using the techniques of section V. In the right panel, we exhibit the correction to this approximation due to the mixed nature of the $(\mathcal{L}, \mathcal{A})$ and $(\mathcal{A}, \mathcal{R})$ sectors by computing the rQFI of the truncated RDM with $n = 3$. Apart from the creation of bound states, the behaviour of the rQFI is qualitatively the same as in the non-interacting case studied in Ref [24]: if we define the rescaled time $\tau = 2t/|A|$, the rQFI grows like τ^2 for $\tau \leq 1$, then decays as $1/\tau$ at late times as the particle escapes the subsystem. Crucially, the rQFI remains $\mathcal{O}(1)$ in the scaling limit at all intermediate times. This confirms that the local quench generates a macroscopic quantum superposition of states whose magnetisations differ by values that diverge linearly in time.

VIII. DISCUSSION: LINK BETWEEN EA AND QFI

In this paper we presented both the QFI and $U(1)$ EA as asymmetry measures, being able to quantify coherence between charge sectors. However, they are not equivalent, and we argue that the relation between them is similar to the one between the variance $\text{Var}(\rho, O)$ of an observable and its Shannon entropy $H(\rho, O) = -\sum_i p_\rho(O_i) \log p_\rho(O_i)$, where $p_\rho(O_i)$ is the probability of the measurement outcome " $O = O_i$ " in the state ρ . For an extensive observable $O = \sum_i o_i$ consisting of local involutions $o_i^2 = I$, it is well-known that [85, 86]

$$H(\rho, O) \leq \frac{1}{2} \log \left[2\pi e \left(\frac{1}{4} \text{Var}(\rho, O) + \frac{1}{12} \right) \right]. \quad (71)$$

When the state ρ is pure, Ref [87] noted that $H(\rho, O)$ precisely corresponds to the entanglement asymmetry $\Delta S(\rho, O)$. For a mixed state $\rho = \sum_i \lambda_i |i\rangle \langle i|$, we can generalise this inequality by applying the Holevo

theorem [81] to the symmetrised state $\mathcal{G}_O(\rho) = \sum_i \lambda_i \mathcal{G}_O(|i\rangle \langle i|)$:

$$S(\mathcal{G}_O(\rho)) + \sum_i \lambda_i \log \lambda_i \leq \sum_i \lambda_i S(\mathcal{G}_O(|i\rangle \langle i|)). \quad (72)$$

The term on the left of the inequality is precisely the entanglement asymmetry associated to the $U(1)$ group generated by O . In the right hand side term, since $|i\rangle$ is pure the Von-Neumann entropy of $\mathcal{G}_O(|i\rangle \langle i|)$ is the shannon entropy associated to O in the state $|i\rangle$, or equivalently the asymmetry $\Delta S(|i\rangle \langle i|, O)$. Therefore, one can apply Eq. (71) which gives

$$\Delta S(\rho, O) \leq \sum_i \lambda_i \frac{1}{2} \log \left[2\pi e(\text{Var}(|i\rangle \langle i|, O^2) + \frac{1}{12}) \right]. \quad (73)$$

Using the concavity of the logarithm, we find

$$\Delta S(\rho, X) \leq \frac{1}{2} \log \left[\sum_i \lambda_i \left(2\pi e(\text{Var}(|i\rangle \langle i|, O^2) + \frac{1}{12}) \right) \right]. \quad (74)$$

This inequality holds for any decomposition $\{\lambda_i, |i\rangle\}$ of the reduced density matrix, in particular for the one that minimises the mean variance $\sum_i \lambda_i \text{Var}(|i\rangle \langle i|, O^2)$. Using now the property that the QFI gives the convex roof of the variance [84, 88], $\frac{1}{4}F_Q(\rho, O) = \inf_{\{\lambda_i, |i\rangle\}} \sum_i \lambda_i \Delta_{|i\rangle \langle i|} O^2$, we finally obtain that

$$\Delta S(\rho, O) \leq \frac{1}{2} \log \left[2\pi e \left(\frac{1}{4}F_Q(\rho, O) + \frac{1}{12} \right) \right]. \quad (75)$$

This inequality could be useful as a lower bound on the QFI. Indeed, we can rewrite it for a subsystem A as

$$\frac{1}{4}F_Q(\rho_A, O_A) \geq \frac{1}{2\pi e} \|O_A\|^{2\Delta S(\rho_A, O_A)} \left(-\frac{1}{12\|O_A\|^2} \right), \quad (76)$$

which automatically implies super-linear scaling of the QFI in the settings where $\Delta S(\rho_A, \|O_A\|) \sim \alpha \log \|O_A\|$ with $\alpha > \frac{1}{2}$, see for instance Ref. [87].

In our setting, this bound is only useful to detect quadratic QFI, i.e. non-zero rescaled QFI $\chi(\rho_A, O_A) = F_Q(\rho_A, O_A)/4\|O_A\|^2$, if the EA has close to maximal value $\Delta S = \log \|O_A\| + \mathcal{O}(1)$. In the free case ($\Delta = 0$), the probability to form a bound state is strictly 0 and the bound (76) can be applied to a quasi-pure subsystem roughly corresponding to the light-cone $A \approx (-t, t)$, where by Eq. (57) $\Delta S(\rho_A, Z_A) \sim \log \|Z_A\| + \mathcal{O}(1)$. In this out-of-equilibrium setting, the bound however becomes non-predictive for the rQFI in the scaling limit as soon as the subsystem becomes mixed, or that the probability to form a bound state is non-zero. This failure is a direct consequence of the form of the probability distribution of the magnetisation, which includes both $\mathcal{O}(1)$ terms and $\mathcal{O}(1/\|O_A\|)$ terms on a support of size $\sim \|O_A\|$, see section VI.

IX. CONCLUSION

In this paper, we investigated the effect of interaction on the rich phenomenology of a local quench on an SSB ground state. We studied this setting by considering the dual XXZ Hamiltonian, which is exactly solvable by coordinate Bethe Ansatz and is analytically tractable after a local quench. We first showed that the domain-wall nature of the excitations amplify quantum interferences, leaving clear imprints of the scattering

phase on the macroscopic profiles of the transverse magnetisation and its correlations. Then, we studied the quantum properties of these correlations under the lens of asymmetry measures, effectively quantifying the coherence between charge sectors of the magnetization. The leading behaviour of both the entanglement asymmetry and QFI can be computed in the limit of large subsystems, showing that subsystems around the light-cone fall in quantum superpositions of a number of magnetisation sectors diverging linearly in time, and that these sectors correspond to macroscopically different magnetisations. Finally, we derived several bounds concerning the EA and QFI, which can be used to greatly simplify the analytical and numerical cost of accessing these quantities thanks to equivalent ones. Since the analysis relies on the two-particle Bethe Ansatz, this framework is very general and can in fact also be applied to non-integrable models, as long as they have kink-like excitations. A natural follow-up to this study would thus be to investigate the effect of integrability breaking within this picture, and in particular to see if this framework can be used to access the Entanglement Asymmetry and Quantum Fisher Information after more general local quenches, that generate a higher number of quasiparticles excitations.

X. AKNOWLEDGEMENTS

I thank Maurizio Fagotti for collaboration on the first stages of the project, as well as Luca Capizzi and Sara Murciano for useful discussions.

Appendix A: Thermodynamic limit for transition amplitudes

We show here the main steps to compute the transition amplitude ${}_s\langle f_1 f_2 | e^{-iHt} | l_1 l_2 \rangle_{s'}$ in the thermodynamic limit. Since $[H, P] = 0$, this amplitude is non-zero only when the two parity sectors match, $s = s'$. The CBA computation of the amplitude in each parity sector is the same as in the XXZ model - see [79] for a comprehensive review - except that i) the elementary excitations are domain walls instead of spin flips and ii) the Bethe equations are modified by the antiperiodic boundary conditions in the $P = -1$ sector.

We start by determining the eigenbasis of H in the $Q = 2$ sector. For a spin chain of size N with periodic boundary conditions, we can construct the eigenstates by considering wavefunctions of the form

$$|k_1 k_2\rangle_s = Z^{(L)}(k_1, k_2) \sum_{l_1 < l_2 = 1/2}^{N-1/2} C_{l_1 l_2}^{k_1 k_2} |l_1 l_2\rangle_s, \text{ with } C_{l_1 l_2}^{k_1 k_2} = S(k_1, k_2) e^{i(k_1 l_1 + k_2 l_2)} + e^{i(k_2 l_1 + k_1 l_2)}. \quad (\text{A1})$$

Solving the eigenvalue equation $H |k_1, k_2\rangle = (\epsilon_{k_1} + \epsilon_{k_2}) |k_1, k_2\rangle$ imposes the expression of the bare energy $\epsilon_k = h - \cos k$ and of the scattering phase,

$$S(k_1, k_2) = -\frac{1 + e^{i(k_1 + k_2)} - 2\Delta e^{ik_1}}{1 + e^{i(k_1 + k_2)} - 2\Delta e^{ik_2}}. \quad (\text{A2})$$

As mentioned in section III, the boundary conditions depend on the parity sector, $|l_1 L + \frac{1}{2}\rangle_{\pm} = \pm |\frac{1}{2}l_1\rangle$. Therefore, so does the Bethe equations which impose the quantisation of the momenta:

$$e^{ik_1 N} = sS(k_1, k_2) \text{ and } e^{-ik_2 N} = sS(k_1, k_2), \quad (\text{A3})$$

where $s = 1$ (resp. -1) in the sector with (anti-)periodic boundary conditions.

We now use the states of Eq. (A1) to write a resolution of the identity in the two-particle sector. One can see that for every solution (k_1, k_2) of the Bethe equations, $S(k_1, k_2) = 1/S(k_2, k_1)$ so $|k_1 k_2\rangle_s$ is colinear with

$|k_2 k_1\rangle_s$. Therefore, writing $\mathcal{B}_s^{(N)}$ the set of solutions of the Bethe equations (A3) the transition amplitude reads

$${}_s\langle f_1 f_2 | e^{-iHt} | l_1 l_2 \rangle_s = \frac{1}{2} \sum_{(k_1, k_2) \in \mathcal{B}_s^{(N)}} |Z^{(N)}(k_1, k_2)|^2 C_{f_1 f_2}^{k_1 k_2} (C_{j_1 j_2}^{k_1 k_2})^* e^{-i(\epsilon_{k_1} + \epsilon_{k_2})t}. \quad (\text{A4})$$

1. Real momenta

We first focus on the solutions $(k_1, k_2) \in \mathbb{R}^2$. For these solutions, the scattering phase has unit modulus, $|S(k_1, k_2)| = 1$, and satisfies $S(k_1, k_2)^{-1} = S(k_1, k_2)^* = S(k_2, k_1)$. We can thus write the term in Eq (A4) as

$$\begin{aligned} C_{f_1 f_2}^{k_1 k_2} (C_{j_1 j_2}^{k_1 k_2})^* &\stackrel{(k_1, k_2) \in \mathbb{R}^2}{=} \left(S(k_1, k_2) e^{i(k_1 f_1 + k_2 f_2)} + e^{i(k_2 f_1 + k_1 f_2)} \right) \times \left(S^*(k_1, k_2) e^{-i(k_1 j_1 + k_2 j_2)} + e^{-i(k_2 j_1 + k_1 j_2)} \right) \\ &= \left[e^{ik_1(f_1 - j_1)} e^{ik_2(f_2 - j_2)} + e^{ik_2(f_1 - j_1)} e^{ik_1(f_2 - j_2)} \right. \\ &\quad \left. + S(k_1, k_2) e^{ik_1(f_1 - j_2)} e^{ik_2(f_2 - j_1)} + S(k_2, k_1) e^{ik_2(f_1 - j_2)} e^{ik_1(f_2 - j_1)} \right]. \quad (\text{A5}) \end{aligned}$$

These terms are however two by two symmetric under the exchange $k_1 \leftrightarrow k_2$, therefore

$$\frac{1}{2} \sum_{(k_1, k_2) \in \mathcal{B}_s^{(N)} \cap \mathbb{R}^2} |Z^{(N)}(k_1, k_2)|^2 C_{f_1 f_2}^{k_1 k_2} (C_{j_1 j_2}^{k_1 k_2})^* e^{-i(\epsilon_{k_1} + \epsilon_{k_2})t} = \sum_{(k_1, k_2) \in \mathcal{B}_s^{(N)} \cap \mathbb{R}^2} |Z^{(N)}(k_1, k_2)|^2 \mathcal{A}_{l_1, l_2 \rightarrow f_1, f_2}^S(k_1, k_2, t), \quad (\text{A6})$$

where

$$\mathcal{A}_{l_1, l_2 \rightarrow f_1, f_2}^S(k_1, k_2, t) = (e^{ik_1(f_1 - j_1)} e^{ik_2(f_2 - j_2)} + S(k_1, k_2) e^{ik_1(f_1 - j_2)} e^{ik_2(f_2 - j_1)}) e^{-i(\epsilon_{k_1} + \epsilon_{k_2})t}. \quad (\text{A7})$$

The normalisation factor is given by

$$\begin{aligned} |Z^{(N)}(k_1, k_2)|^{-2} &= \sum_{l_1 < l_2 = 1/2}^{N-1/2} |C_{l_1 l_2}^{k_1 k_2} (C_{l_1 l_2}^{k_1 k_2})^*|^2 \\ &= N^2 \left[1 + \frac{1}{N} \frac{1 - \cos(k_1 - k_2) - \cos(k_2 - k_1 - \theta_{k_1 k_2}) - \cos \theta_{k_1 k_2}}{\cos(k_1 - k_2) - 1} + \frac{1}{N^2} \frac{\cos(k_1 N - k_2 N + \theta_{k_1 k_2}) + \cos \theta_{k_1 k_2}}{\cos(k_1 - k_2) - 1} \right] \\ &= N^2 \left[1 + \frac{1}{N} \frac{1 - \cos(k_1 - k_2) - \cos(k_2 - k_1 - \theta_{k_1 k_2}) - \cos \theta_{k_1 k_2}}{\cos(k_1 - k_2) - 1} + \frac{1}{N^2} \frac{\cos(3\theta_{k_1 k_2}) + \cos \theta_{k_1 k_2}}{\cos(k_1 - k_2) - 1} \right], \quad (\text{A8}) \end{aligned}$$

where $e^{i\theta_{k_1 k_2}} = S(k_1, k_2)$ and we imposed the Bethe equations (A3) to obtain the last line. We take the latter to be the definition of $Z^{(N)}(k_1, k_2)$. The sum (A6) can be carried out explicitly exploiting the fact that the total momentum is conserved. Indeed, making the following change of variables: $\kappa = \frac{1}{2}(k_1 + k_2)$ and $\delta = \frac{1}{2}(k_1 - k_2)$, the Bethe equations can be rewritten as

$$(e^{i\kappa N} = s \text{ and } e^{i\delta N} = S_\kappa(\delta)) \text{ or } (e^{i\kappa N} = -s \text{ and } e^{i\delta N} = -S_\kappa(\delta)), \quad (\text{A9})$$

where $S_\kappa(\delta) = S(\kappa + \delta, \kappa - \delta)$. From this new set of Bethe Equations it is clear that κ admits the same quantisation as a free model with either periodic or antiperiodic boundary conditions. The domain of

integration $k_1, k_2 \in (-\pi, \pi)$ translates to $\kappa \in (-\pi, \pi)$ and $\delta \in (-\pi + |\kappa|, \pi - |\kappa|)$. All the difficulty lies in selecting the δ solutions of Eq. (A9) in that domain, which can be done using a residue theorem. Indeed,

$$\begin{aligned} & \sum_{(k_1, k_2) \in \mathcal{B}_s^{(N)} \cap \mathbb{R}^2} |Z^{(N)}(k_1, k_2)|^2 \mathcal{A}_{l_1, l_2 \rightarrow f_1, f_2}^S(k_1, k_2, t) \\ &= \lim_{\epsilon \rightarrow 0} \sum_{n=1}^N \frac{1}{2\pi i} \oint_{\gamma_\epsilon(\kappa_n^+)} |Z^{(N)}(\kappa_n^+ + \delta, \kappa_n^+ - \delta)|^2 \frac{siNe^{i\delta N} - \partial_\delta S_{\kappa_n^+}(\delta)}{se^{i\delta N} - S_{\kappa_n^+}(\delta)} \mathcal{A}_{l_1, l_2 \rightarrow f_1, f_2}^S(\kappa_n^+ + \delta, \kappa_n^+ - \delta, t) d\delta \\ &+ \lim_{\epsilon \rightarrow 0} \sum_{n=1}^N \frac{1}{2\pi i} \oint_{\gamma_\epsilon(\kappa_n^-)} |Z^{(N)}(\kappa_n^- + \delta, \kappa_n^- - \delta)|^2 \frac{siNe^{i\delta N} + \partial_\delta S_{\kappa_n^-}(\delta)}{se^{i\delta N} + S_{\kappa_n^-}(\delta)} \mathcal{A}_{l_1, l_2 \rightarrow f_1, f_2}^S(\kappa_n^- + \delta, \kappa_n^- - \delta, t) d\delta, \quad (\text{A10}) \end{aligned}$$

where $\kappa_n^+ = \frac{2\pi n}{L}$, $\kappa_n^- = \frac{2\pi(n+1/2)}{L}$ and the contour is given by

$$\gamma_\epsilon(\kappa) : -\pi + |\kappa| - i\epsilon \rightarrow \pi - |\kappa| - i\epsilon \rightarrow \pi - |\kappa| + i\epsilon \rightarrow -\pi + |\kappa| + i\epsilon \rightarrow \pi - |\kappa| + i\epsilon. \quad (\text{A11})$$

Taking the thermodynamic limit $N \rightarrow \infty$, the integrand on the interval $-\pi + |\kappa| + i\epsilon \rightarrow \pi - |\kappa| + i\epsilon$ vanishes as $N \rightarrow \infty$ like $1/N^2$, while on the interval $-\pi + |\kappa| - i\epsilon \rightarrow \pi - |\kappa| - i\epsilon$ it simplifies to $|Z_{\kappa_n^+}^{(N)}(\delta)|^2 (siNe^{i\delta N} - \partial_\delta S_{\kappa_n^+}(\delta)) / (se^{i\delta N} - S_{\kappa_n^+}(\delta)) \rightarrow i/N$. Taking the limit $N \rightarrow \infty$ then $\epsilon \rightarrow 0$ in the sum gives

$$\begin{aligned} \lim_{N \rightarrow \infty} \sum_{(k_1, k_2) \in \mathcal{B}_s^{(N)} \cap \mathbb{R}^2} |Z^{(N)}(k_1, k_2)|^2 \mathcal{A}_{l_1, l_2 \rightarrow f_1, f_2}^S(k_1, k_2, t) &= \lim_{\epsilon \rightarrow 0} \sum_{n=1}^N \frac{1}{2\pi N} \int_{-\pi + |\kappa| + i\epsilon}^{\pi - |\kappa| + i\epsilon} d\delta \mathcal{A}_{l_1, l_2 \rightarrow f_1, f_2}^S(\kappa_n^+ + \delta, \kappa_n^+ - \delta, t) \\ &+ \lim_{\epsilon \rightarrow 0} \sum_{n=1}^N \frac{1}{2\pi N} \int_{-\pi + |\kappa| + i\epsilon}^{\pi - |\kappa| + i\epsilon} d\delta \mathcal{A}_{l_1, l_2 \rightarrow f_1, f_2}^S(\kappa_n^- + \delta, \kappa_n^- - \delta, t), \quad (\text{A12}) \end{aligned}$$

independantly of the parity sector. Finally, we can simplify these sums using the Euler-Maclaurin formula:

$$\lim_{N \rightarrow +\infty} \sum_{(k_1, k_2) \in \mathcal{B}_s^{(N)} \cap \mathbb{R}^2} |Z^{(N)}(k_1, k_2)|^2 \mathcal{A}_{l_1, l_2 \rightarrow f_1, f_2}^S(k_1, k_2, t) = \lim_{\epsilon \rightarrow 0} \frac{1}{\pi} \int_{-\pi}^{\pi} d\kappa \int_{-\pi + |\kappa| + i\epsilon}^{\pi - |\kappa| + i\epsilon} d\delta \mathcal{A}_{l_1, l_2 \rightarrow f_1, f_2}^S(\kappa + \delta, \kappa - \delta, t). \quad (\text{A13})$$

By changing back to the original variables and keeping the $+i\epsilon$ regularisation implicit, we simply have

$$\lim_{N \rightarrow +\infty} \sum_{(k_1, k_2) \in \mathcal{B}_s^{(N)} \cap \mathbb{R}^2} |Z^{(N)}(k_1, k_2)|^2 \mathcal{A}_{l_1, l_2 \rightarrow f_1, f_2}^S(k_1, k_2, t) = \frac{1}{4\pi^2} \int_{-\pi}^{\pi} dk_1 dk_2 \mathcal{A}_{l_1, l_2 \rightarrow f_1, f_2}^S(k_1, k_2, t). \quad (\text{A14})$$

2. Complex momenta

We now consider complex solutions $(k_1, k_2) \notin \mathbb{R}^2$. If the momenta have non-zero imaginary part, the Bethe equations imply that either $S(k_1, k_2)$ or $S(k_2, k_1)$ is exponentially small in N . Consequently, the solutions must have the form

$$(k_1, k_2) = \left(\frac{K}{2} + i\eta, \frac{K}{2} - i\eta \right) + \mathcal{O}(e^{-N}), \quad (\text{A15})$$

with $K, \eta \in \mathbb{R}$. For momenta of this form, the term $C_{f_1 f_2}^{k_1 k_2} (C_{j_1 j_2}^{k_1 k_2})^*$ takes the form

$$\begin{aligned} C_{f_1 f_2}^{k_1 k_2} (C_{j_1 j_2}^{k_1 k_2})^* &=_{(k_1, k_2) = (\frac{K}{2} + i\eta, \frac{K}{2} - i\eta)} \left(S(k_1, k_2) e^{i(k_1 f_1 + k_2 f_2)} + e^{i(k_2 f_1 + k_1 f_2)} \right) \times \left(S(k_1, k_2) e^{i(k_1 j_1 + k_2 j_2)} + e^{i(k_2 j_1 + k_1 j_2)} \right)^* \\ &= e^{iK(\frac{f_1 + f_2}{2} - \frac{j_1 + j_2}{2})} \left[S\left(\frac{K}{2} + i\eta, \frac{K}{2} - i\eta\right) e^{\eta(f_2 - f_1)} + e^{-\eta(f_2 - f_1)} \right] \left[S\left(\frac{K}{2} + i\eta, \frac{K}{2} - i\eta\right) e^{\eta(j_2 - j_1)} + e^{-\eta(j_2 - j_1)} \right]. \end{aligned} \quad (\text{A16})$$

In the thermodynamic limit, the physical solutions should stay normalisable. Therefore, to avoid divergence as $f_2 - f_1 \rightarrow \infty$ they should correspond to $S(K/2 + i\eta, K/2 - i\eta) = 0$ (fixing $\eta > 0$), which imposes the value of η as a function of K :

$$e^{-\eta(K)} = \frac{\cos(K/2)}{\Delta}, \text{ and } \cos K/2 \leq \Delta. \quad (\text{A17})$$

The bound state contributions are thus given by

$$C_{f_1 f_2}^{k_1 k_2} (C_{j_1 j_2}^{k_1 k_2})^* \Big|_{(k_1, k_2) = (\frac{K}{2} + i\eta, \frac{K}{2} - i\eta)} = e^{iK(\frac{f_1 + f_2}{2} - \frac{j_1 + j_2}{2})} e^{-\eta(f_2 - f_1 + j_2 - j_1)}, \quad (\text{A18})$$

and the normalisation factor is

$$\begin{aligned} |Z(K/2 + i\eta, K/2 - i\eta)|^{-2} &= \sum_{f_1 < f_2 = 1/2}^{N-1/2} |C_{f_1 f_2}^{k_1 k_2}|^2 \\ &= \sum_{f_1 < f_2 = 1/2}^{N-1/2} e^{-2\eta(f_2 - f_1)} = \sum_{f_1=1}^N e^{-2\eta} \frac{1 - e^{-2\eta(N-f_1)}}{1 - e^{-2\eta}} = \frac{N}{e^{2\eta} - 1} + \mathcal{O}(1). \end{aligned} \quad (\text{A19})$$

Finally, using the Euler-Maclaurin formula we find that

$$\begin{aligned} \lim_{N \rightarrow \infty} \sum_{(k_1, k_2) \in \mathcal{B}_s^{(N)} \setminus \mathbb{R}^2} |Z^{(N)}(k_1, k_2)|^2 C_{f_1 f_2}^{k_1 k_2} (C_{j_1 j_2}^{k_1 k_2})^* \\ = \frac{1}{\pi} \int_0^\pi dK (e^{2\eta(K)} - 1) e^{iK(\frac{f_1 + f_2}{2} - \frac{j_1 + j_2}{2})} e^{-\eta(K)(f_2 - f_1 + j_2 - j_1)} e^{-iE_K t}. \end{aligned} \quad (\text{A20})$$

Appendix B: Scaling limits

In this appendix, we show how to obtain the scaling limit of $p_{(X, Y)}(t)$

1. Scattering states contribution

The contribution of the scattering states can be expressed as

$$\begin{aligned}
p_{(X,Y)} &= \langle \psi(t) | \Pi_X^Y | \psi(t) \rangle = \sum_{\substack{f_1 \in X \\ f_2 \in Y \\ f_1 < f_2}} |\psi_{f_1 f_2}(t)|^2 \\
&= \sum_{\substack{f_1 \in X \\ f_2 \in Y \\ f_1 < f_2}} \frac{1}{(2\pi)^4} \left(\int_{-\pi}^{\pi} dk_1 dk_2 dp_1 dp_2 \tilde{\psi}(k_1, k_2) \tilde{\psi}^*(p_1, p_2) e^{i[f_1(k_1 - p_1) + f_2(k_2 - p_2) - (\epsilon_{k_1} + \epsilon_{k_2} - \epsilon_{p_1} - \epsilon_{p_2})t]} \right). \quad (\text{B1})
\end{aligned}$$

The terms of this sum are symmetric under the exchange $f_1 < f_2$. Therefore, we can separate it between the intersection $X \cap Y$ and the disjoint union $X \setminus Y$ and $Y \setminus X$ as

$$\langle \psi(t) | \Pi_X^Y | \psi(t) \rangle = \sum_{\substack{f_1 \in X \setminus Y \\ f_2 \in Y \setminus X}} |\psi_{f_1 f_2}(t)|^2 + \frac{1}{2} \sum_{f_1, f_2 \in X \cap Y} |\psi_{f_1 f_2}(t)|^2 - \frac{1}{2} \sum_{f \in X \cap Y} |\psi_{ff}(t)|^2. \quad (\text{B2})$$

By Lieb-Robinson bounds and stationary phase, the last term is a sum of $\mathcal{O}(t)$ terms of order $\mathcal{O}(t^{-2})$ and is therefore vanishing in the scaling limit. Consequently, the two relevant terms can be expressed as $\sum_{f_1 \in A, f_2 \in B} |\psi_{f_1 f_2}(t)|^2$. If we note $A = \llbracket a_l, a_r \rrbracket$ and $B = \llbracket b_l, b_r \rrbracket$, we can explicitly carry out the geometric sums:

$$\begin{aligned}
\sum_{\substack{f_1 \in A \\ f_2 \in B}} |\psi_{f_1 f_2}(t)|^2 &= \int_{-\pi}^{\pi} \frac{dk_1 dk_2 dp_1 dp_2}{(2\pi)^4} \left(\tilde{\psi}(k_1, k_2) \tilde{\psi}^*(p_1, p_2) \right. \\
&\quad \left. \frac{e^{ia_l(p_1 - k_1)} - e^{ia_r(p_1 - k_1)}}{1 - e^{i(k_1 - p_1)}} \frac{e^{ib_l(k_2 - p_2)} - e^{ib_r(k_2 - p_2)}}{1 - e^{i(k_2 - p_2)}} e^{-i(\epsilon_{k_1} + \epsilon_{k_2} - \epsilon_{p_1} - \epsilon_{p_2})t} \right). \quad (\text{B3})
\end{aligned}$$

The integrand is finite at $k_1 = p_1$ and $k_2 = p_2$, but diverges in the scaling limit as $|A|, |B| \rightarrow \infty$. Therefore, if we define the new set of variables $\kappa_{1,2} = (k_{1,2} + p_{1,2})/2$ and $\delta_{1,2} = (k_{1,2} - p_{1,2})/2$ we can expand the integrand around $\delta_1, \delta_2 \sim 0$:

$$\begin{aligned}
\sum_{\substack{f_1 \in A \\ f_2 \in B}} |\psi_{f_1 f_2}(t)|^2 &= \frac{1}{\pi^2} \int_{-\pi}^{\pi} d\kappa_1 d\kappa_2 |\tilde{\psi}(\kappa_1, \kappa_2)|^2 \\
&\quad \times \int_{-\pi+|\kappa_1|}^{\pi-|\kappa_1|} d\delta_1 \frac{e^{it\delta_1[a_l/t - \epsilon'_{\kappa_1}]} - e^{it\delta_1[a_r/t - \epsilon'_{\kappa_1}]}}{-i\delta_1} \int_{-\pi+|\kappa_2|}^{\pi-|\kappa_2|} d\delta_2 \frac{e^{it\delta_2[b_l/t - \epsilon'_{\kappa_2}]} - e^{it\delta_2[b_r/t - \epsilon'_{\kappa_2}]}}{-i\delta_2} + \mathcal{O}(t^{-1}), \quad (\text{B4})
\end{aligned}$$

where we discarded the derivative $\partial_{k_1} S(k_1, k_2) \ll t$ in the scaling limit as a $\mathcal{O}(t^{-1})$ correction. The integrands do not diverge at $\delta_1, \delta_2 \rightarrow 0$. Therefore, we can sum the principal values of the individual terms:

$$\mathcal{P} \int_{-\pi+|\kappa|}^{\pi-|\kappa|} d\delta \frac{e^{it\delta x}}{-i\delta} = - \int_{-\pi+|\kappa|}^{\pi-|\kappa|} d\delta \frac{\sin(t\delta x)}{\delta}. \quad (\text{B5})$$

Using now the change of variable $\Lambda = t\delta$, we get

$$-\int_{-\pi+|\kappa|}^{\pi-|\kappa|} d\delta \frac{\sin(t\delta x)}{\delta} \underset{t \rightarrow \infty}{=} -\int_{-\infty}^{+\infty} d\Lambda \frac{\sin(\Lambda x)}{\Lambda} = -\pi \operatorname{sgn}(x). \quad (\text{B6})$$

Inserting Eq. (B6) into Eq. (B4) yields

$$\sum_{\substack{f_1 \in A \\ f_2 \in B}} |\psi_{f_1 f_2}(t)|^2 = \frac{1}{4\pi^2} \int_{-\pi}^{\pi} d\kappa_1 d\kappa_2 |\tilde{\psi}(\kappa_1, \kappa_2)|^2 \theta(f_1/t - a_l) \theta(a_r - f_1/t) \theta(f_2/t - b_l) \theta(b_r - f_2/t). \quad (\text{B7})$$

2. Bound states contribution

The contribution of the bound states, whose wavefunction is given by

$$\nu_{f_1, f_2} = \frac{1}{\pi} \int_0^\pi dK \tilde{\nu}_{f_2 - f_1}(K) e^{iK \frac{f_1 + f_2}{2}} e^{-iE_K t}, \quad (\text{B8})$$

reads

$$\begin{aligned} p_{(X, Y)}^B &= \langle \nu(t) | \Pi_X^Y | \nu(t) \rangle = \sum_{\substack{f_1 \in X \\ f_2 \in Y \\ f_1 < f_2}} |\nu_{f_1 f_2}(t)|^2 \\ &= \sum_{\substack{f_1 \in X \\ f_2 \in Y \\ f_1 < f_2}} \frac{1}{(2\pi)^4} \left(\int_{-\pi}^{\pi} dK dP \tilde{\nu}_{f_2 - f_1}(K) \tilde{\nu}_{f_2 - f_1}(P) e^{i[f_1(k_1 - p_1) + f_2(k_2 - p_2) - (\epsilon_{k_1} + \epsilon_{k_2} - \epsilon_{p_1} - \epsilon_{p_2})t]} \right). \end{aligned} \quad (\text{B9})$$

We can again separate the sum between $X \setminus Y$, $Y \setminus X$ and $X \cap Y$. Because of the exponential decay of $\tilde{\nu}_{f_2 - f_1}(K)$ with $f_2 - f_1$, if $f_1 \in X \setminus Y$ and $f_2 \in Y \setminus X$ the contribution goes to zero in the scaling limit. The only non-zero contribution is given by

$$p_{(X, Y)}^B \approx \sum_{\substack{f_1, f_2 \in X \cap Y \\ f_1 < f_2}} \frac{1}{(2\pi)^2} \left(\int_{-\pi}^{\pi} dK dP \tilde{\nu}_{f_2 - f_1}(K) \tilde{\nu}_{f_2 - f_1}(P) e^{i[(K - P)(f_1 + f_2)/2 - (E_K - E_P)t]} \right). \quad (\text{B10})$$

Up to exponentially small corrections in time, we can write

$$\begin{aligned} p_{(X, Y)}^B &\approx \sum_{f_1 \in X \cap Y} \sum_{r=1}^{+\infty} \frac{1}{(2\pi)^2} \left(\int_{-\pi}^{\pi} dK dP \tilde{\nu}_r(K) \tilde{\nu}_r(P) e^{i[(K - P)(f_1 + r/2) - (E_K - E_P)t]} \right) \\ &= \sum_{r=1}^{+\infty} \frac{1}{(2\pi)^2} \left(\int_{-\pi}^{\pi} dK dP \tilde{\nu}_r(K) \tilde{\nu}_r(P) \frac{e^{il(K - P)} - e^{ir(K - P)}}{1 - e^{i(K - P)}} e^{i[(K - P)r/2 - (E_K - E_P)t]} \right) \end{aligned} \quad (\text{B11})$$

Making the change of variable $K = \tilde{K} + \delta$, $P = \tilde{K} - \delta$ we expand around the main contribution at $\delta \sim 0$:

$$p_{(X, Y)}^B \approx \sum_{r=1}^{+\infty} \frac{1}{(2\pi)^2} \left(\int_{-\pi}^{\pi} d\tilde{K} \int d\delta |\nu_r(\tilde{K})|^2 \frac{e^{it\delta[l/t - E'_K]} - e^{it\delta[r/t - E'_K]}}{-i\delta} \right). \quad (\text{B12})$$

Using now that

$$\sum_{r=1}^{+\infty} |\nu_r(\tilde{K})|^2 = 1 - e^{-2\eta(\tilde{K})d_0}, \quad (\text{B13})$$

we finally find

$$\underline{p}_{(\mathcal{X}, \mathcal{Y})}^B = \frac{1}{(2\pi)} \left(\int_{-\pi}^{\pi} d\tilde{K} (1 - e^{-2\eta(\tilde{K})d_0}) \Theta[E'_{\tilde{K}} \in \mathcal{X} \cap \mathcal{Y}] \right). \quad (\text{B14})$$

Appendix C: Bounds on QFI

1. From truncated RDM

Consider a (normalised) density matrix acting on a Hilbert space of dimension D (D can be infinite) $\rho = \sum_{j=1}^D \lambda_j |j\rangle \langle j|$ with eigenvalues organised in decreasing order, $\forall j \lambda_j \geq \lambda_{j+1}$. Even if ρ is rank R with $R < D$, it admits such an expression where $\lambda_i = 0$ for $i > R$. The QFI of ρ with respect to an observable \mathcal{O} is given by

$$\frac{1}{4} F_Q(\rho, \mathcal{O}) = \frac{1}{2} \sum_{i,j=1}^D \frac{(\lambda_i - \lambda_j)^2}{\lambda_i + \lambda_j} |\langle i | \mathcal{O} | j \rangle|^2. \quad (\text{C1})$$

The term $\frac{(\lambda_i - \lambda_j)^2}{\lambda_i + \lambda_j}$ tends to 0 when $\lambda_i, \lambda_j \rightarrow 0$ but not when only one of the eigenvalues is set to zero, therefore the double sum spans the full Hilbert space. Separating zero from non-zero eigenvalues and inserting a resolution of the identity, we can re-express this identity as a sum over non-zero eigenvalues of the density matrix:

$$\frac{1}{4} F_Q(\rho, \mathcal{O}) = \sum_{i=1}^R \lambda_i \langle i | \mathcal{O}^2 | i \rangle - 2 \sum_{i,j=1}^R \frac{\lambda_i \lambda_j}{\lambda_i + \lambda_j} |\langle i | \mathcal{O} | j \rangle|^2. \quad (\text{C2})$$

Let us now truncate ρ keeping only its n largest eigenvalues, and write $\rho = (1 - \epsilon_n)\rho^{(n)} + \epsilon_n \delta \rho^{(n)}$, with $(1 - \epsilon_n)\rho^{(n)} = \sum_{i=1}^n \lambda_i |i\rangle \langle i|$ and $\epsilon_n \delta \rho^{(n)} = \sum_{i=n+1}^D \lambda_i |i\rangle \langle i|$. Because of the convexity properties of the QFI,

$$\frac{1}{4} F_Q(\rho, \mathcal{O}) \leq \frac{1}{4} (1 - \epsilon_n) F_Q(\rho^{(n)}, \mathcal{O}) + \epsilon_n \|\mathcal{O}\|^2, \quad (\text{C3})$$

where we used the fact that $\frac{1}{4} F_Q(\sigma, \mathcal{O})$ is bounded by the square of the norm of \mathcal{O} , $\|\mathcal{O}\|^2$, for any density matrix σ .

Let us now construct a lower bound for $F_Q(\rho, \mathcal{O})$ from $F_Q(\rho^{(n)}, \mathcal{O})$. We can see from Eq. (C7) that

$$\frac{1}{4} F_Q(\rho, \mathcal{O}) = \frac{1}{4} (1 - \epsilon_n) F_Q(\rho^{(n)}, \mathcal{O}) + \frac{1}{4} \epsilon_n F_Q(\delta \rho^{(n)}, \mathcal{O}) - 4 \sum_{i=1}^n \sum_{j=n+1}^R \frac{\lambda_i \lambda_j}{\lambda_i + \lambda_j} |\langle i | \mathcal{O} | j \rangle|^2. \quad (\text{C4})$$

Using now that $F_Q(\sigma, \mathcal{O}) \geq 0$, $\lambda_i \lambda_j / (\lambda_i + \lambda_j) \leq \lambda_j$ and $|\langle i | \mathcal{O} | j \rangle|^2 \leq \|\mathcal{O}\|^2$, we finally find that

$$\frac{1}{4} F_Q(\rho, \mathcal{O}) \geq \frac{1}{4} (1 - \epsilon_n) F_Q(\rho^{(n)}, \mathcal{O}) - 4n \epsilon_n \|\mathcal{O}\|^2. \quad (\text{C5})$$

2. From variance

When a density matrix is almost pure, it is useful to similarly bound the QFI from the variance of the state. To that end, let us re-express the QFI as

$$\frac{1}{4}F_Q(\rho, \mathcal{O}) = \text{Var}(\rho, \mathcal{O}) + \sum_{i,j=1}^R \lambda_i \lambda_j \langle i | \mathcal{O} | i \rangle \langle j | \mathcal{O} | j \rangle - 2 \sum_{i,j=1}^R \frac{\lambda_i \lambda_j}{\lambda_i + \lambda_j} |\langle i | \mathcal{O} | j \rangle|^2. \quad (\text{C6})$$

Doing the same procedure as in the previous subsection with $n = 1$ (we only keep the largest eigenvalue), we find that

$$\begin{aligned} \frac{1}{4}F_Q(\rho, \mathcal{O}) = \text{Var}(\rho, \mathcal{O}) + \lambda_1^2 \langle 1 | \mathcal{O} | 1 \rangle^2 - \lambda_1 \langle 1 | \mathcal{O} | 1 \rangle^2 + 2\lambda_1 \langle 1 | \mathcal{O} | 1 \rangle \sum_{j=2}^R \lambda_j \langle j | \mathcal{O} | j \rangle \\ - 4 \sum_{j=2}^R \frac{\lambda_1 \lambda_j}{\lambda_1 + \lambda_j} |\langle 1 | \mathcal{O} | j \rangle|^2 - 2 \sum_{i,j=2}^R \frac{\lambda_i \lambda_j}{\lambda_i + \lambda_j} |\langle i | \mathcal{O} | j \rangle|^2. \end{aligned} \quad (\text{C7})$$

Using now again the inequality $\lambda_1 \lambda_j / (\lambda_1 + \lambda_j) \leq \lambda_j$, and $2 \sum_{i,j=2}^R \frac{\lambda_i \lambda_j}{\lambda_i + \lambda_j} |\langle i | \mathcal{O} | j \rangle|^2 \leq \text{Tr}(\delta \rho^{(1)} \mathcal{O}^2) \leq \epsilon_1 \|\mathcal{O}\|^2$, we get

$$\frac{1}{4}F_Q(\rho, \mathcal{O}) \geq \text{Var}(\rho, \mathcal{O}) + (\epsilon_1^2 - 2\epsilon_1 + \epsilon_1 - 2(1 - \epsilon_1)\epsilon_1 - 4\epsilon_1 - \epsilon_1) \|\mathcal{O}\|^2, \quad (\text{C8})$$

or the simpler bound

$$\frac{1}{4}F_Q(\rho, \mathcal{O}) \geq \text{Var}(\rho, \mathcal{O}) - 8\epsilon_1 \|\mathcal{O}\|^2. \quad (\text{C9})$$

This bound presents the advantage of not requiring any spectral analysis of the density matrix, since also ϵ_1 can be bounded by the purity of the density matrix. Therefore,

$$\frac{1}{4}F_Q(\rho, \mathcal{O}) \geq \text{Var}(\rho, \mathcal{O}) - 8 \left(1 - \sqrt{\text{Tr} \rho^2}\right) \|\mathcal{O}\|^2. \quad (\text{C10})$$

Appendix D: Fourier coefficients of the scattering phase in XXZ model

Since $S(k_1, k_2)$ is a bounded function appearing only as a kernel on a compact domain (i.e. $[-\pi, \pi]^2$), one can represent it in Fourier basis:

$$S(k_1, k_2) \equiv \sum_{nm \in \mathbb{Z}} S_{nm} e^{ik_1 n} e^{ik_2 m} \quad (\text{D1})$$

Let us recall the explicit expression of the scattering phase and recast it as

$$S(k_1, k_2) = -e^{i(k_1 - k_2)} \frac{e^{-ik_1} + e^{ik_2} - 2\Delta}{e^{ik_1} + e^{-ik_2} - 2\Delta} \quad (\text{D2})$$

1. $\Delta > 1$:

Since $|e^{ik_1} + e^{-ik_2}| \leq 2$, one can easily obtain the Fourier coefficients by expanding

$$S(k_1, k_2) = -e^{i(k_1 - k_2)} \frac{e^{-ik_1} + e^{ik_2} - 2\Delta}{e^{ik_1} + e^{-ik_2} - 2\Delta} = \frac{e^{i(k_1 - k_2)}}{2\Delta} (e^{-ik_1} + e^{ik_2} - 2\Delta) \sum_{j=0}^{+\infty} \left(\frac{e^{ik_1} + e^{-ik_2}}{2\Delta} \right)^j, \quad (\text{D3})$$

which gives

$$S_{jp} = \frac{(j - j^2 + p + (4\Delta^2 - 2)jp - p^2)}{(-j + j^2 - p + 2jp + p^2)} (2\Delta)^{-(j+p)} \binom{j+p}{j} \quad (\text{D4})$$

2. $\Delta < 1$:

When $\Delta < 1$, the most convenient way to obtain the Fourier coefficients of the scattering phase is to compute the integral

$$S_{nm} = \frac{1}{4\pi^2} \int_{-\pi}^{\pi} dk_1 dk_2 S(k_1, k_2) e^{-i(k_1 n + k_2 m)} \quad (\text{D5})$$

using residue theorem. First of all, notice that the imaginary part of the integrand is odd for $k_1, k_2 \in \mathbb{R}$. Therefore, the Fourier coefficients are real. Let us now make the change of variable $K = \frac{k_1 + k_2}{2}$ and $\delta = \frac{k_2 - k_1}{2}$. We have

$$S_{nm} = \frac{1}{\pi^2} \int_0^{\pi} d\kappa \int_{-\pi+\kappa}^{\pi-\kappa} d\delta \operatorname{Re} \left(S_{\kappa}(\delta) e^{-i\kappa(n+m)} e^{-i\delta(n-m)} \right), \quad (\text{D6})$$

where

$$S_{\kappa}(\delta) = S(\kappa + \delta, \kappa - \delta) = S(\kappa + \delta, \kappa - \delta) = -\frac{\cos \kappa - \Delta e^{i\delta}}{\cos \kappa - \Delta e^{-i\delta}}. \quad (\text{D7})$$

We can now evaluate (D6) by deforming the contour of integration of δ using residue theorem. The scattering phase satisfies

$$S_{\kappa}(\pi - \kappa + i\eta) e^{-i(\pi - \kappa + i\eta)(n-m)} = (S_{\kappa}(-\pi + \kappa + i\eta) e^{-i(-\pi + \kappa + i\eta)(n-m)})^* \quad (\text{D8})$$

therefore

$$\operatorname{Re} \left(\int_{-\pi+\kappa}^{-\pi+\kappa+i\Lambda} d\delta S_{\kappa}(\delta) e^{-i\kappa(n+m)} e^{-i\delta(n-m)} + \int_{\pi-\kappa+i\Lambda}^{\pi-\kappa} d\delta S_{\kappa}(\delta) e^{-i\kappa(n+m)} e^{-i\delta(n-m)} \right) = 0. \quad (\text{D9})$$

This allows to rewrite (D6) as

$$S_{nm} = -\frac{1}{\pi^2} \int_0^{\pi} d\kappa e^{-i\kappa(n+m)} \left[\int_{-\pi+\kappa+i\Lambda}^{\pi-\kappa+i\Lambda} d\delta \operatorname{Re} \left(S_{\kappa}(\delta) e^{-i\delta(n-m)} \right) + 2\pi i \operatorname{sgn} \Lambda R_{\Lambda}(\kappa) \right], \quad (\text{D10})$$

where $R_\Lambda(\kappa)$ is the sum of the residues of $S_\kappa(\delta)e^{-i\delta(n-m)}$ in the contour $-\pi + \kappa \rightarrow \pi - \kappa \rightarrow \pi - \kappa + i\Lambda \rightarrow -\pi + \kappa + i\Lambda \rightarrow -\pi + \kappa$. The latter are located at $\delta_\kappa = i \ln(|\cos \kappa/\Delta|) + \frac{1+\text{sgn}(\cos \kappa/\Delta)}{2}\pi$ (modulo 2π). Therefore,

$$R_\Lambda = i \theta\left(\frac{\cos \kappa}{\Delta}\right) \theta(|\Lambda| - |\text{Im } \delta_\kappa|) \Theta[\text{sgn}(\Lambda)] = \text{sgn } \text{Im } \delta_\kappa \left[\left(\frac{\cos \kappa}{\Delta}\right)^{n-m-2} - \left(\frac{\cos \kappa}{\Delta}\right)^{n-m} \right]. \quad (\text{D11})$$

Taking the contour with $\Lambda_\kappa = \text{sgn}[(\cos K - \Delta)(n - m + 1)]\infty$ (with $\text{sgn}(0) = 1$ by convention), we find that

$$S(k_1, k_2) = e^{ik_1 - ik_2} \sum_{mn} (\lambda_{m+n}^{m-n+1} - \lambda_{m+n}^{m-n-1}) e^{-ik_1 m} e^{-ik_2 n}, \quad (\text{D12})$$

where

$$\lambda_m^n = \frac{2 \text{sgn}(m)}{\pi} \int_0^{\pi/2} dK \left(\frac{\Delta}{\cos K}\right)^m \cos(nK) \theta[\text{sgn}(m)(\cos K - \Delta)]. \quad (\text{D13})$$

[1] D. M. Greenberger, M. A. Horne, and A. Zeilinger, Going Beyond Bell's Theorem, in *Bell's Theorem, Quantum Theory and Conceptions of the Universe*, edited by M. Kafatos (Springer Netherlands, Dordrecht, 1989) pp. 69–72.

[2] E. Schrödinger, Die gegenwärtige Situation in der Quantenmechanik, *Naturwissenschaften* **23**, 844 (1935).

[3] J. D. Trimmer, The present situation in quantum mechanics: A translation of Schrödinger's "Cat Paradox" paper, *Proceedings of the American Philosophical Society*, 323 (1980).

[4] W.-B. Gao, C.-Y. Lu, X.-C. Yao, P. Xu, O. Gühne, A. Goebel, Y.-A. Chen, C.-Z. Peng, Z.-B. Chen, and J.-W. Pan, Experimental demonstration of a hyper-entangled ten-qubit Schrödinger cat state, *Nature Physics* **6**, 331–335 (2010).

[5] A. Omran, H. Levine, A. Keesling, G. Semeghini, T. T. Wang, S. Ebadi, H. Bernien, A. S. Zibrov, H. Pichler, S. Choi, *et al.*, Generation and manipulation of Schrödinger cat states in Rydberg atom arrays, *Science* **365**, 570 (2019).

[6] C. Song, K. Xu, H. Li, Y.-R. Zhang, X. Zhang, W. Liu, Q. Guo, Z. Wang, W. Ren, J. Hao, *et al.*, Generation of multicomponent atomic Schrödinger cat states of up to 20 qubits, *Science* **365**, 574 (2019).

[7] G. D. Fresco, B. Spagnolo, D. Valenti, and A. Carollo, Multiparameter quantum critical metrology, *SciPost Phys.* **13**, 077 (2022).

[8] G. Di Fresco, B. Spagnolo, D. Valenti, and A. Carollo, Metrology and multipartite entanglement in measurement-induced phase transition, *Quantum* **8**, 1326 (2024).

[9] Y. Chen, S. Murciano, P. Sala, and J. Alicea, Quantum sensing with critical systems: impact of symmetry, imperfections, and decoherence (2026), arXiv:2601.04364 [quant-ph].

[10] V. Zauner, M. Ganahl, H. G. Evertz, and T. Nishino, Time evolution within a comoving window: scaling of signal fronts and magnetization plateaus after a local quench in quantum spin chains, *Journal of Physics: Condensed Matter* **27**, 425602 (2015).

[11] V. Eisler and F. Maislinger, Front dynamics in the XY chain after local excitations, *SciPost Phys.* **8**, 037 (2020).

[12] G. Delfino and M. Sorba, Space of initial conditions and universality in nonequilibrium quantum dynamics, *Nuclear Physics B* **983**, 115910 (2022).

[13] S. Bocini and M. Fagotti, Growing Schrödinger's cat states by local unitary time evolution of product states, *Physical Review Research* **6**, 10.1103/physrevresearch.6.033108 (2024).

[14] T. Antal, Z. Rácz, A. Rákos, and G. M. Schütz, Transport in the XX chain at zero temperature: Emergence of flat magnetization profiles, *Physical Review E* **59**, 4912–4918 (1999).

[15] S. Scopa and D. Karevski, Scaling of fronts and entanglement spreading during a domain wall melting, *The European Physical Journal Special Topics* **232**, 1763–1781 (2023).

- [16] V. Eisler, Domain-wall melting and entanglement in free-fermion chains with a band structure, *SciPost Physics Core* **8**, 10.21468/scipostphyscore.8.4.069 (2025).
- [17] K. Bidzhiev, M. Fagotti, and L. Zadnik, Macroscopic Effects of Localized Measurements in Jammed States of Quantum Spin Chains, *Physical Review Letters* **128**, 10.1103/physrevlett.128.130603 (2022).
- [18] M. Fagotti, Quantum Jamming Brings Quantum Mechanics to Macroscopic Scales, *Physical Review X* **14**, 10.1103/physrevx.14.021015 (2024).
- [19] V. Hunyadi, Z. Rácz, and L. Sasvári, Dynamic scaling of fronts in the quantum XX chain, *Physical Review E* **69**, 10.1103/physreve.69.066103 (2004).
- [20] M. Collura, A. De Luca, and J. Viti, Analytic solution of the domain-wall nonequilibrium stationary state, *Physical Review B* **97**, 10.1103/physrevb.97.081111 (2018).
- [21] V. Eisler and Z. Rácz, Full Counting Statistics in a Propagating Quantum Front and Random Matrix Spectra, *Physical Review Letters* **110**, 10.1103/physrevlett.110.060602 (2013).
- [22] V. Marić, F. Ferro, and M. Fagotti, Disorder-order interface propagating over the ferromagnetic ground state in the transverse field Ising chain, *Physical Review B* **111**, 205118 (2025).
- [23] V. Marić, F. Ferro, and M. Fagotti, Macroscopic Quantum States and Universal Correlations in a Disorder-Order Interface Propagating over a 1D Ground State, *Physical Review Letters* **134**, 236302 (2025).
- [24] F. Ferro and M. Fagotti, Kicking Quantum Fisher Information out of Equilibrium (2025), arXiv:2503.21905 [quant-ph].
- [25] S. Sachdev and A. P. Young, Low Temperature Relaxational Dynamics of the Ising Chain in a Transverse Field, *Phys. Rev. Lett.* **78**, 2220 (1997).
- [26] H. Rieger and F. Iglói, Semiclassical theory for quantum quenches in finite transverse Ising chains, *Physical Review B* **84**, 10.1103/physrevb.84.165117 (2011).
- [27] K. Korzekwa, *Resource theory of asymmetry*, Ph.D. thesis, Imperial College London (2013).
- [28] I. Marvian and R. W. Spekkens, How to quantify coherence: Distinguishing speakable and unspeakable notions, *Physical Review A* **94**, 10.1103/physreva.94.052324 (2016).
- [29] I. Marvian, R. W. Spekkens, and P. Zanardi, Quantum speed limits, coherence, and asymmetry, *Physical Review A* **93**, 10.1103/physreva.93.052331 (2016).
- [30] K. Yamaguchi and H. Tajima, Beyond i.i.d. in the Resource Theory of Asymmetry: An Information-Spectrum Approach for Quantum Fisher Information, *Physical Review Letters* **131**, 10.1103/physrevlett.131.200203 (2023).
- [31] C. Zhang, B. Yadin, Z.-B. Hou, H. Cao, B.-H. Liu, Y.-F. Huang, R. Maity, V. Vedral, C.-F. Li, G.-C. Guo, and D. Girolami, Detecting metrologically useful asymmetry and entanglement by a few local measurements, *Physical Review A* **96**, 10.1103/physreva.96.042327 (2017).
- [32] G. Gour, Resources of the Quantum World (2024), arXiv:2402.05474 [quant-ph].
- [33] J. Åberg, Quantifying Superposition (2006), arXiv:quant-ph/0612146 [quant-ph].
- [34] F. Ares, S. Murciano, and P. Calabrese, Entanglement asymmetry as a probe of symmetry breaking, *Nature Communications* **14**, 10.1038/s41467-023-37747-8 (2023).
- [35] F. Ares, P. Calabrese, and S. Murciano, The quantum Mpemba effects (2025), arXiv:2502.08087 [cond-mat.stat-mech].
- [36] S. Murciano, F. Ares, I. Klich, and P. Calabrese, Entanglement asymmetry and quantum Mpemba effect in the XY spin chain, *Journal of Statistical Mechanics: Theory and Experiment* **2024**, 013103 (2024).
- [37] K. Chalas, F. Ares, C. Rylands, and P. Calabrese, Multiple Crossings during Dynamical Symmetry Restoration and Implications for the Quantum Mpemba Effect, *Journal of Statistical Mechanics: Theory and Experiment* **2024**, 103101.
- [38] S. Yamashika, F. Ares, and P. Calabrese, Entanglement asymmetry and quantum Mpemba effect in two-dimensional free-fermion systems, *Phys. Rev. B* **110**, 085126 (2024).
- [39] H. Yu, S. Liu, and S.-X. Zhang, Quantum Mpemba effects from symmetry perspectives, *AAPPS Bulletin* **35**, 10.1007/s43673-025-00157-7 (2025).
- [40] G. Teza, J. Bechhoefer, A. Lasanta, O. Raz, and M. Vucelja, Speedups in nonequilibrium thermal relaxation: Mpemba and related effects, *Physics Reports* **1164**, 1–97 (2026).
- [41] Y.-H. Yu, T.-R. Jin, L. Zhang, K. Xu, and H. Fan, Tuning the quantum Mpemba effect in an isolated system by initial-state engineering, *Physical Review B* **112**, 10.1103/yzjd-pk8h (2025).
- [42] S. Liu, H.-K. Zhang, S. Yin, S.-X. Zhang, and H. Yao, Symmetry restoration and quantum Mpemba effect in many-body localization systems, *Science Bulletin* **70**, 3991–3996 (2025).

[43] X. Turkeshi, P. Calabrese, and A. D. Luca, Quantum Mpemba Effect in Random Circuits (2024), arXiv:2405.14514 [quant-ph].

[44] T. Banerjee, S. Das, and K. Sengupta, Entanglement asymmetry in periodically driven quantum systems (2025), arXiv:2412.03654 [quant-ph].

[45] F. Ares, V. Vitale, and S. Murciano, Quantum Mpemba effect in free-fermionic mixed states, *Physical Review B* **111**, 10.1103/physrevb.111.104312 (2025).

[46] F. Caceffo, S. Murciano, and V. Alba, Entangled multiplets, asymmetry, and quantum Mpemba effect in dissipative systems, *Journal of Statistical Mechanics: Theory and Experiment* **2024**, 063103 (2024).

[47] C. Rylands, E. Vernier, and P. Calabrese, Dynamical Symmetry Restoration in the Heisenberg Spin Chain, *Journal of Statistical Mechanics: Theory and Experiment* **2024**, 123102.

[48] K. Klobas, Non-Equilibrium Dynamics of Symmetry-Resolved Entanglement and Entanglement Asymmetry: Exact Asymptotics in Rule 54*, *Journal of Physics A: Mathematical and Theoretical* **57**, 505001.

[49] B. J. J. Khor, D. M. Kürkçüoglu, T. J. Hobbs, G. N. Perdue, and I. Klich, Confinement and Kink Entanglement Asymmetry on a Quantum Ising Chain, *Quantum* **8**, 1462 (2024).

[50] B. Bertini, K. Klobas, M. Collura, P. Calabrese, and C. Rylands, Dynamics of charge fluctuations from asymmetric initial states, *Physical Review B* **109**, 10.1103/physrevb.109.184312 (2024).

[51] F. Ferro, F. Ares, and P. Calabrese, Non-equilibrium entanglement asymmetry for discrete groups: the example of the XY spin chain, *Journal of Statistical Mechanics: Theory and Experiment* **2024**, 023101 (2024).

[52] A. Russotto, F. Ares, and P. Calabrese, Non-Abelian entanglement asymmetry in random states, *Journal of High Energy Physics* **2025**, 1 (2025).

[53] F. Benini, V. Godet, and A. H. Singh, Entanglement Asymmetry in Conformal Field Theory and Holography, *Progress of Theoretical and Experimental Physics* **2025**, 10.1093/ptep/ptaf080 (2025).

[54] H.-H. Chen and Z.-J. Tang, Entanglement asymmetry in the Hayden-Preskill protocol (2025), arXiv:2411.17695 [hep-th].

[55] Y. Kusuki, S. Murciano, H. Ooguri, and S. Pal, Entanglement asymmetry and symmetry defects in boundary conformal field theory, *Journal of High Energy Physics* **2025**, 10.1007/jhep01(2025)057 (2025).

[56] M. Fossati, F. Ares, J. Dubail, and P. Calabrese, Entanglement asymmetry in CFT and its relation to non-topological defects, *Journal of High Energy Physics* **2024**, 10.1007/jhep05(2024)059 (2024).

[57] L. Capizzi and M. Mazzoni, Entanglement asymmetry in the ordered phase of many-body systems: the Ising Field Theory (2023), arXiv:2307.12127 [cond-mat.stat-mech].

[58] F. Ares, S. Murciano, P. Calabrese, and L. Piroli, Entanglement asymmetry dynamics in random quantum circuits, *Physical Review Research* **7**, 10.1103/m3np-p5xj (2025).

[59] L. K. Joshi, J. Franke, A. Rath, F. Ares, S. Murciano, F. Kranzl, R. Blatt, P. Zoller, B. Vermersch, P. Calabrese, C. F. Roos, and M. K. Joshi, Observing the Quantum Mpemba Effect in Quantum Simulations, *Phys. Rev. Lett.* **133**, 010402 (2024).

[60] Y. Xu, C.-P. Fang, B.-J. Chen, M.-C. Wang, Z.-Y. Ge, Y.-H. Shi, Y. Liu, C.-L. Deng, K. Zhao, Z.-H. Liu, T.-M. Li, H. Li, Z. Wang, G.-H. Liang, D. Feng, X. Guo, X.-Y. Gu, Y. He, H.-T. Liu, Z.-Y. Mei, Y. Xiao, Y. Yan, Y.-H. Yu, W.-P. Yuan, J.-C. Zhang, Z.-A. Wang, G. Liu, X. Song, Y. Tian, Y.-R. Zhang, S.-X. Zhang, K. Huang, Z. Xiang, D. Zheng, K. Xu, and H. Fan, Observation and Modulation of the Quantum Mpemba Effect on a Superconducting Quantum Processor (2025), arXiv:2508.07707 [quant-ph].

[61] R. Takagi, Skew Informations from an Operational View via Resource Theory of Asymmetry, *Scientific Reports* **9**, 14562 (2019).

[62] Y. Kusuki, S. Pal, and H. Tajima, Resource-Theoretic Quantifiers of Weak and Strong Symmetry Breaking: Strong Entanglement Asymmetry and Beyond (2026), arXiv:2601.20924 [hep-th].

[63] S. Yamashita, S. Endo, and H. Tajima, Quantum Fisher Information as a Measure of Symmetry Breaking in Quantum Many-Body Systems (2025), arXiv:2509.07468 [cond-mat.stat-mech].

[64] K. C. Tan, V. Narasimhachar, and B. Regula, Fisher Information Universally Identifies Quantum Resources, *Phys. Rev. Lett.* **127**, 200402 (2021).

[65] L. Pezzé and A. Smerzi, Entanglement, Nonlinear Dynamics, and the Heisenberg Limit, *Phys. Rev. Lett.* **102**, 100401 (2009).

[66] P. Hyllus, W. Laskowski, R. Krischek, C. Schwemmer, W. Wieczorek, H. Weinfurter, L. Pezzé, and A. Smerzi, Fisher information and multiparticle entanglement, *Phys. Rev. A* **85**, 022321 (2012).

[67] G. Tóth, Multipartite entanglement and high-precision metrology, *Phys. Rev. A* **85**, 022322 (2012).

- [68] F. Fröwis and W. Dür, Measures of macroscopicity for quantum spin systems, *New Journal of Physics* **14**, 093039 (2012).
- [69] I. Frerot and T. Roscilde, Quantum variance: A measure of quantum coherence and quantum correlations for many-body systems, *Phys. Rev. B* **94**, 075121 (2016).
- [70] J. Lambert and E. S. Sørensen, Estimates of the quantum Fisher information in the antiferromagnetic Heisenberg spin chain with uniaxial anisotropy, *Physical Review B* **99**, 10.1103/physrevb.99.045117 (2019).
- [71] W. Zhong, J. Liu, J. Ma, and X.-G. Wang, Quantum Fisher information and spin squeezing in one-axis twisting model, *Chinese Physics B* **23**, 060302 (2014).
- [72] Z. Jiang, Quantum Fisher information for states in exponential form, *Physical Review A* **89**, 10.1103/physreva.89.032128 (2014).
- [73] Y. Gao and H. Lee, Bounds on quantum multiple-parameter estimation with Gaussian state, *The European Physical Journal D* **68**, 10.1140/epjd/e2014-50560-1 (2014).
- [74] D. Šafránek, A. R. Lee, and I. Fuentes, Quantum parameter estimation using multi-mode Gaussian states (2015), arXiv:1502.07924 [quant-ph].
- [75] E. P. Wigner and M. M. Yanase, INFORMATION CONTENTS OF DISTRIBUTIONS, *Proceedings of the National Academy of Sciences* **49**, 910 (1963), <https://www.pnas.org/doi/pdf/10.1073/pnas.49.6.910>.
- [76] A. Rath, C. Branciard, A. Minguzzi, and B. Vermersch, Quantum Fisher Information from Randomized Measurements, *Phys. Rev. Lett.* **127**, 260501 (2021).
- [77] P. Hauke, M. Heyl, L. Tagliacozzo, and P. Zoller, Measuring multipartite entanglement through dynamic susceptibilities, *Nature Physics* **12**, 778–782 (2016).
- [78] L. Zadnik, K. Bidzhiev, and M. Fagotti, The folded spin-1/2 XXZ model: II. Thermodynamics and hydrodynamics with a minimal set of charges, *SciPost Physics* **10**, 10.21468/scipostphys.10.5.099 (2021).
- [79] F. Franchini, *An Introduction to Integrable Techniques for One-Dimensional Quantum Systems* (Springer International Publishing, 2017).
- [80] E. H. Lieb and D. W. Robinson, The finite group velocity of quantum spin systems, *Commun. Math. Phys.* **28**, 251 (1972).
- [81] M. A. Nielsen and I. L. Chuang, *Quantum Computation and Quantum Information: 10th Anniversary Edition* (Cambridge University Press, 2010).
- [82] C. Holzhey, F. Larsen, and F. Wilczek, Geometric and renormalized entropy in conformal field theory, *Nuclear Physics B* **424**, 443–467 (1994).
- [83] P. Calabrese and J. Cardy, Entanglement entropy and quantum field theory, *Journal of Statistical Mechanics: Theory and Experiment* **2004**, P06002 (2004).
- [84] S. Yu, Quantum Fisher Information as the Convex Roof of Variance (2013), arXiv:1302.5311 [quant-ph].
- [85] J. L. Massey, in *Information Theory: Proceedings of the 1988 Beijing International Workshop on Information Theory (BIWIT'88)* (Pergamon, 1989) july 4–7, 1988.
- [86] T. M. Cover, *Elements of information theory* (John Wiley & Sons, 1999).
- [87] M. Mazzoni, L. Capizzi, and L. Piroli, Breaking global symmetries with locality-preserving operations (2025), arXiv:2508.15892 [quant-ph].
- [88] G. Tóth and D. Petz, Extremal properties of the variance and the quantum Fisher information, *Physical Review A* **87**, 10.1103/physreva.87.032324 (2013).